PHASE TRANSITION
IN
HOMOGENEOUS FLOW
OF NEMATIC FLUIDS

by

İVET BAHAR

B.S. in Ch.E., Boğaziçi University, 1980

Submitted to the Institute for Graduate Studies in
Science and Engineering in partial fulfillment of

the requirements for the degree of

Master of Science

in

Chemical Engineering

Boğaziçi University
1983

Approved by:

Doç. Dr. Burak ERMAN
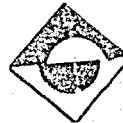(Thesis Supervisor)

Doç. Dr. Salih DİNÇER
(Thesis Supervisor)

Doç.Dr. Amable Hortaçsu

2. June, 1983

ACKNOWLEDGEMENTS

ABSTRACT

Possibility of formation of a highly concentrated anisotropic phase in a dilute solution of rodlike molecules is investigated. The free energy expression for quiescent solutions of rodlike particles, introduced by Flory, is extended to the case where the molecules are subject to homogeneous velocity field. An additional term accounting for the contribution of the flow field to phase transition is incorporated into the free energy expression. The contribution of stress-induced diffusion is considered too. It is concluded that there will be a highly concentrated liquid crystalline phase deposition on the stagnant regions of the conduit, provided that the solvent-solute interaction is sufficiently high. The application of the theory to the aggregation of cholesterol molecules, in blood vessels, is discussed.

ÖZET

Flory'nin çubuksu cisimler içeren çözeltiler için tanımladığı serbest enerji denklemi, homojen bir akışın etkisini de kapsayacak şekilde genelleştirilmiştir. Moleküllerin gerilimi en düşüğe indirmek eğilimlerinden doğan diffüzyon gözönüne alınarak, durgun bölgelerdeki muhtemel derişik anizotropik evre oluşması incelenmiştir. Pozitif bir enerji-etkileşme parametresinin katkısı olduğu takdirde, belirli bölgelerde sıvı kristal bir evre belireceği tespit edilmiştir. Matematiksel modellemenin damardaki kolesterol birikimini bir ölçüde açıklaması tartışılmıştır.

TABLE OF CONTENTS

LIST OF FIGURES

I. INTRODUCTION TO ANISOTROPIC FLUIDS

In this chapter, various ordered fluid mesophases, commonly called liquid crystals, are described, with particular attention being given to the nature of molecular ordering. Also, some of the factors influencing the phase transition from isotropic liquid to ordered fluid, are explained, as an introduction, to understand the behaviour of anisotropic fluids.

1.1   MESOPHASES

Many organic materials exhibit more than a single transition in passing from liquid to solid, necessitating the existence of intermediate phases, known as "mesophases". There are two main groups of mesophases: (Priestley, et.al, 1975).

i) Disordered crystal mesophases, commonly called plastic crystals, which retain a three dimensional crystal lattice but are characterized by substantial rotational disorder, due to the fact that beyond a critical temperature, the molecules are energetic enough to overcome rotational energy barrier, but are not energetic enough to break up the lattice so that they are transitionally well ordered.

ii) Ordered fluid mesophases, referred to as "liquid crystals",
most often composed of elongated molecules; they are charac-
terized by their lack of crystal lattice together with some
degree of rotational order. As a result, they posses simul-
taneously liquidlike (fluidity) and solidlike (molecular
order) character.

1.2 MAIN TYPES AND PROPERTIES OF LIQUID CRYSTALS

To generate a liquid crystal, one must use elongated objects,
referred to as the "building blocks" (P.G. de Gennes, 1974). This may
be achieved using either small organic molecules, such as p-azoxyanisole
(PAA), N-p-methoxybenzylidene p-butylaniline (MBBA), cholesterol esters
or synthetic polypeptides in suitable solvents, some standard examples
including deoxyribonucleic acid (DNA), tobacco mosaic virus (TMV).

Phase transition from amorphous to anisotropic state takes place
either by increasing the concentration of the rodlike entities in solvent-
solute systems, or by varying the temperature as in the case of thermo-
tropic liquid crystals. In thermotropic systems, most widely encountered
in the case of pure systems, the arrangement of the molecules are deter-
mined by the van der Waals attractions between pairs of neighbouring
molecules, touching each other. Though, recently, the theory of phase
equilibria in thermotropic liquid crystalline systems, has been extended
to the case where the rods are dispersed in a diluent, thermotropic systems
occur most readily, with pure compounds in view of the fact that the van
deer Waals force of attraction between molecules come into play when the
molecules are closer together. These attractive force will have a more
pronounced effect at lower temperatures because the molecules will have

lower velocities and hence, will be within interacting distances of one another for longer periods of time.

In the study that follows, solvent-solute systems, whose transitions are most naturally effected by increasing the concentration of the solute will be treated. The effect of increase in concentration is reflected as:

    i)   increase in electrokinetic and electrostatic interactions in the case of <u>lyotropic liquid crystals</u>

   ii)   competition for space, in the case of solutions of relatively longer rodlike particles that cannot interpenetrate each other.

Lyotropic liquid crystals are mixtures of amphiphilic compounds (Winsor and Gray, 1974), and a polar solvent most frequently water. Aggregates of amphiphilic molecules in aqueous solution, always form in such a manner as to reduce the hydrophobic interaction between their hydrocarbon tails and the water, while simultaneously maximizing the hydrophilic interactions of their polar heads with the aqueous solvent. As a result, they acquire lamellar structure (referred to as the neat phase or gel phase) or give rise to the formation of spherical and cylindrical micelles. According to R-theory of fused micellar phases (Winsor, 1974) the ratio R which is a measure of the relative tendency of the amphiphilic layer to become convex towards its lipophilic environment compared to that of it to become convex to its polar environment, is equal to unity so that the lamellae retain their parallel and planar arrangement. With certain binary aqueous neat phase, dilution beyond a certain limit leads to a discontinuous phase transition producing an isotropic solution. The breakdown of the gel phase is associated with the

tendency of dilution to decrease R below unity, because with increasing dilution, the tendency of the amphiphilic layer to become convex to water is relatively increased. The stability of the gel phase may eventually be maintained by some internal rearrangement (i.e. the average micellar form approaches spherical) so as to increase the interfacial area per polar group. However, on further dilution, the spherical micelles too, are dissociated and join the isotropic phase. It is emphasized that all the effects of dilution considered above are reversible, thus commencing with a dilute disordered solution and progressively increasing the concentration, lamellar loci appear within the isotropic solution, resulting in the separation of the anisotropic phase, finally.

As stated above, increase in concentration, induces phase transition not only with amphiphilic solute molecules, but in the case of non amphiphilic, rigid, highly asymmetrical molecules dispersed in a diluent, where the only interparticle force is in the form of steric repulsion, associated with the accomodation in a limited volume. The behaviour of this group constitutes the main subject of this thesis. The statistical theory of phase separation in such systems of rodlike particles, will be fully explained in Chapter 2.

1.3   CLASSIFICATION ACCORDING TO MOLECULAR ORDER

The classification distinguishes three major classes: the nematic, the cholesteric, and the smectic.

1.3.1 Nematic Order

In nematic order, the molecules tend to align parallel to each other, in the direction of a common axis, ñ, the director. Nematic phases occur

only with materials which do not distinguish between right and left, with no dipole moment, and which are not ionizable. A schematic representation of the nematic order is shown in Fig. 1.1.
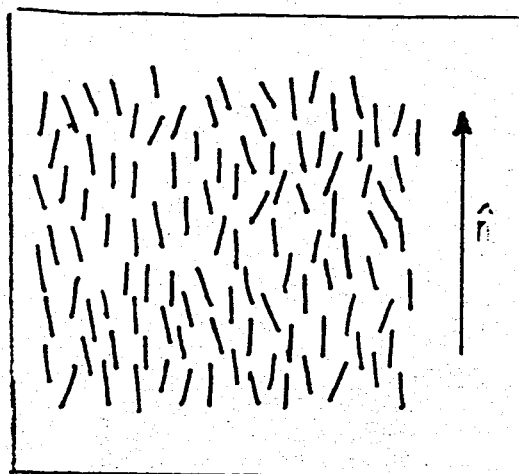
FIGURE 1.1 - The arrangement of molecules in the nematic
mesophase

1.3.2 Cholesteric Order

If we dissolve, in a nematic liquid a molecule which is chiral (i.e. different of its mirror image), we find out that the structure undergoes a helical distortion, common to cholesterol esters. On a local scale, cholesteric and nematic ordering are very similar. However, in cholesteric order, the director ñ, is not constant in space, but rotates from plane to plane. In other terms, the structure of a cholesteric liquid crystal is periodic with a spatial period L, equal to one half of the pitch. A schematic representation of cholesteric order is shown in Fig. 1.2.
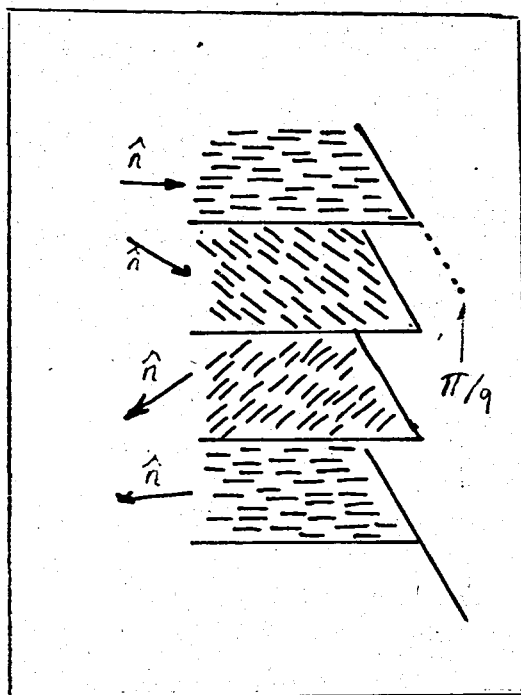
FIGURE 1.2 - Schematic representation of cholesteric mesophase

1.3.3 Smectic Order

Smectics are layered structures with a well-defined interlayer spacing. In the case of smectic A, the layer thickness is identically equal to the full molecular length; there is a substantial probability for interlayer diffusion, while in smectic C, there is a uniform tilting of the molecular axes with respect to the layer normal, resulting in interlayer diffusion of lower probability.

In this work, solutions exhibiting a nematic order will be considered. Cholesterol order occurs with chiral systems; smectic order is most frequently observed with amphiphilic compounds. As to the nematic order, it occurs when the system is achiral or a racemic mixture of right and left handed species. Since, the mesogens considered in this work will be rigid rodlike, non-ionizable, non-polar particles, nematic ordering will be prevailing in the anisotropic phase.
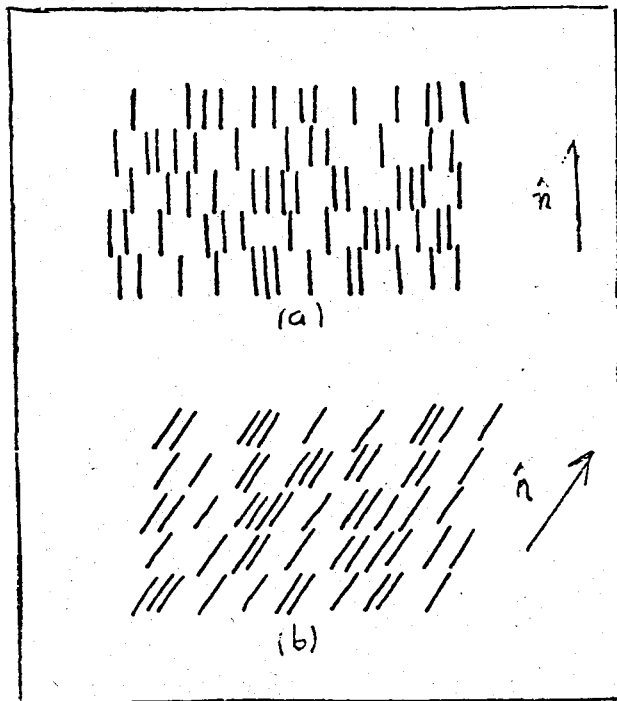
FIGURE 1.3 - Schematic representation of two types of smectic
order (a) smectic A order, (b) smectic C order.

II. PHASE EQUILIBRIA IN SOLUTIONS OF RODLIKE PARTICLES

The precipitation of rodlike particles in quiescent solutions was explained by Flory (1956), through the use of a statistical mechanical approach based on a modified lattice model. As can be predicted from this theory, separation into an isotropic and a somewhat more concentrated anisotropic phase arises as a consequence of particle asymmetry. In what follows, an outline of the theory of phase equilibria in solutions of rodlike particles will be presented.

2.1. EQUILIBRIUM DEGREE OF DISORDER

By making use of a partition function for a system of rigid rodlike particles with partial orientation about an axis, Flory (1956) derived a general expression for the free energy of mixing as a function of the mole numbers the axis ratio x (or length to width ratio) and a disorientation parameter y. The final expression has the form (See Appendix A1 for detailed derivation):

$$\frac{\Delta G_m}{kT} = n_1 \ln v_1 + n_2 \ln v_2 - (n_1 + y n_2)\ln[1 - v_2(1 - y/x)]$$

$$- n_2[\ln(xy^2) - y + 1] + \chi_1 x n_2 v_1 \qquad (2.1)$$

where

v_1, v_2 = volume fractions of the solvent and solute, respectively;

n_1, n_2 = number of molecules of solvent and solute;

X_1 = dimensionless solvent-solute interaction parameter;

k = Boltzmann constant;

T = absolute temperature.

Since, no external restraints apply to y, it will be assumed to adopt the value which minimizes ΔG_m. Hence, we differentiate Eq. (2.1) with respect to y, at constant x, n_2, n_1 and T, and equate to zero

$$\frac{\partial \Delta G_m}{\partial y}\bigg|_{x,n_1,n_2} = -(n_1 + yn_2)\left[\frac{v_2/x}{1 - v_2(1 - y/x)}\right] - n_2 \ln(1 - v_2(1 - y/x))$$

$$- n_2\left[\frac{2xy}{xy^2}\right] + n_2 = 0 \qquad (2.2)$$

Substituting $n_1 = x(v_1/v_2)n_2$ and rearranging, we obtain

$$v_2 = \frac{x}{x - y} \; 1 - \exp\{-\frac{2}{y}\} \qquad (2.3)$$

or

$$\ln(1 - v_2(1 - y/x)) = -2/y \qquad (2.4)$$

Hence the y that minimizes ΔG_m is the one that satisfies Eq. (2.3). By making use of Eq. (2.3) one can find the possible set of (v_2, y), that are most stable for a given x. Among this set, there is a pair (v_2^*, y^*) corresponding to minimum solute fraction, together with maximum disorientation parameter, for stable anisotropy. This pair is obtainable by differentiating Eq. (2.3) with respect to y and equating to zero, so that:

$$v_2^* = 1 - (1 - 2/y^*)\exp\{-\frac{2}{y^*}\} \qquad (2.5)$$

and

$$y^* = \frac{1}{2}(x - 1) - (\frac{1}{3} y^* + \frac{1}{6} y^{*2} + \ldots\ldots) \qquad (2.6)$$

For $v_2 < v_2^*$, ΔG_m decreases monotonically with y, hence a necessary condition for existence of stable anisotropic phase is $v_2 > v_2^*$. However for values of v_2, slightly above v_2^*, there is a metastable region, where $\Delta G_{m_{anisotropic}} > \Delta G_{m_{isotropic}}$. In both cases, ΔG_m is calculated from Eq. (2.1), only using $y = x$ (See Appendix A2) for the case of isotropic liquid. Calculations show that this metastable region is rather small.

In the absence of diluent ($v_2 = 1$), according to Eq. (2.5), $y = 2$. Substituting these values in Eq. (2.3) we get $x = 2e = 5.44$ as the minimum value of x required for a stable anisotropic state for the pure solute (Flory, 1956). Hence, a length to width ratio of about $2e$ is sufficient to cause spontaneous ordering of the phase, for a pure system. For particles in solution, the critical x value increases with dilution, if the system is athermal ($X_1 = 0$). For non-athermal solutions, the properties change drastically and will be considered later.

2.2 CHEMICAL POTENTIAL

By substituting Eq. (2.3) in Eq. (2.1) the following more convenient expression is obtained for the free energy of formation of the phase with equilibrium disorder:

$$\frac{\Delta G_m}{kT} = n_1 \ln v_1 + n_2 \ln v_2 + \frac{2n_1}{y} - n_2[\ln(xy^2) - y - 1]$$

$$+ X_1 x n_2 v_1 \qquad (2.7)$$

where y is given by Eq. (2.3).

The chemical potential of a solvent in solution relative to that of the solvent as a pure component, may be obtained by differentiating ΔG_m with respect to n_1. If the n's represent the number of moles instead of molecules, we may write:

$$\frac{1}{N} \partial(\frac{\Delta G_m}{kT})/\partial n_1 = \frac{\mu_1 - \mu_1^0}{RT}$$

where N = Avogadro's number;

μ_i = chemical potential of component i in solution

μ_i^0 = chemical potential of pure compound i.

Then,

$$\frac{\mu_1 - \mu_1^0}{RT} = \frac{\partial(n_1 \ln v_1)}{\partial n_1} + \frac{\partial(n_2 \ln v_2)}{\partial n_1} + \frac{2}{y} - \{\frac{2n_1}{y^2}\}(\frac{dy}{dn_1})_{eq}$$

$$+ \{n_2(\frac{dy}{dn_1})_{eq} + n_2(\frac{2xy}{xy^2})(\frac{dy}{dn_1})_{eq}\} + \frac{\partial(\chi_1 xn_2 v_1)}{\partial n_1} \qquad (2.8)$$

$$\frac{\partial n_1 \ln v_1}{\partial n_1} = n_1 \frac{\partial \ln v_1}{\partial n_1} + \ln v_1 \frac{\partial n_1}{\partial n_1} = \ln v_1 + n_1 \frac{\partial \ln v_1}{\partial n_1}$$

but $$\frac{\partial v_1}{\partial n_2} = \frac{\partial[n_1/(n_1 + xn_2)]}{\partial n_1} = \frac{n_1 + xn_2 - n_1}{(n_1 + xn_2)^2} - \frac{v_2}{xn_2}$$

$$\frac{\partial(n_1 \ln v_1)}{\partial n_1} = \ln(1 - v_2) + v_2 \qquad (2.9)$$

$$\frac{\partial(n_2 \ln v_2)}{\partial n_1} = n_2 \frac{\partial \ln v_2}{\partial n_1} = \frac{n_2 \; \partial v_2/v_2}{\partial n_1} = \frac{n_2}{v_2} \frac{\partial v_2}{\partial n_1}$$

but

$$\frac{\partial v_2}{\partial n_1} = \frac{\partial[xn_2/(xn_2 + n_1)]}{\partial n_1} = \frac{v_2^2}{xn_2}$$

$$\frac{\partial(n_2 \ln v_2)}{\partial n_1} = \frac{n_2}{v_2}[\frac{v_2^2}{xn_2}] = \frac{v_2}{x} \tag{2.10}$$

$$\frac{\partial(\chi_1 x \; n_2 v_1)}{\partial n_1} = \chi_1 x \; n_2 \frac{\partial v_1}{\partial n_1} = \chi_1 v_2^2 \tag{2.11}$$

Inserting Eqs. (2.9), (2.10), (2.11) in Eq. (2.8), we obtain,

$$\frac{\mu_1 - \mu_1^o}{RT} = \ln(1 - v_2) + (1 - 1/x)v_2 + \frac{2}{y}$$

$$+ (n_2 - \frac{2n_1}{y} - \frac{2n_2}{y})(\frac{dy}{dn_1})_{eq} \tag{2.12}$$

Also evaluation of $(dy/dn_1)_{eq}$ from Eq. (2.3) yields, finally,

$$\frac{\mu_1 - \mu_1^o}{RT} = \ln(1 - v_2) + \frac{y - 1}{x}v_2 + \frac{2}{y} + \chi_1 v_2^2 \tag{2.13}$$

This equation represents the chemical potential for the anisotropic phase. As to the chemical potential of the isotropic phase, it is given by the well-known equation (Flory, 1953):

$$\frac{\mu_1 - \mu_1^o}{RT}\bigg|_{y=x} = \ln(1 - v_2) + (1 - \frac{1}{x})v_2 + \chi_1 v_2^2 \tag{2.14}$$

Similarly, the chemical potentials for the solute in nematic and disordered phase are given by Equations (2.15) and (2.16), respectively.

$$\frac{\mu_2 - \mu_2^0}{RT} = \ln\left(\frac{v_2}{x}\right) + (y - 1)v_2 + 2 - \ln y^2 + \chi_1 x(1 - v_2)^2 \quad (2.15)$$

$$\left.\frac{\mu_2 - \mu_2^0}{RT}\right|_{y=x} = \ln\left(\frac{v_2}{x}\right) + (x - 1)v_2 - \ln x^2 + \chi_1 x(1 - v_2)^2 \quad (2.16)$$

Chemical potentials calculated from Eq. (2.13) to (2.16) in conjunction with Eq. (2.3) are shown in Fig. 2.1.
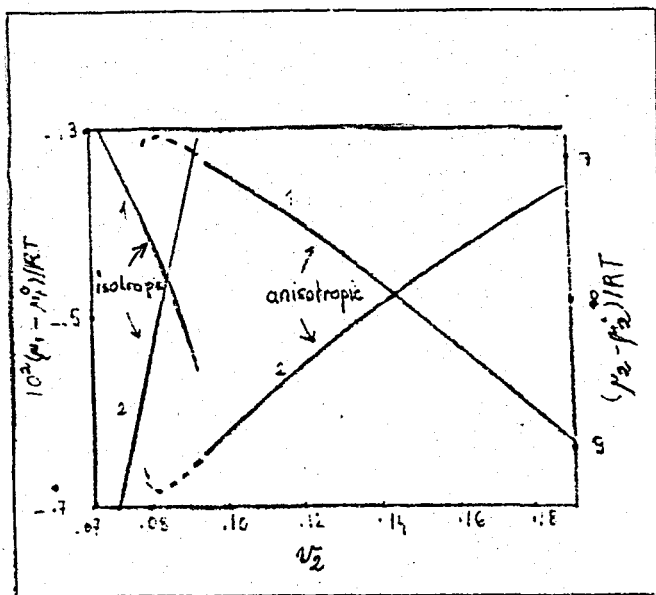
Solvent: '1', left-hand ordinate scale

Solute : '2', right-hand ordinate scale

Region of metastable order are shown by broken lines.

FIGURE 2.1 - Chemical potentials for $X_1 = 0$ and $x = 100$

The calculations were carried out, for $x = 100$, by Flory. The curves for isotropic solutions are valid up to $v_2 = 0.0935$ of absolute stability. Then a discontinuity corresponding to metastable region is

observed. For higher solute volume fractions, nematic and isotropic phases coexist.

Similar calculations were done to find out the chemical potentials, for $x = 20$. The limit of absolute stability was found to be equal to $v_2 = 0.4354$, by using the following procedure: the isotropic curve must be continued until reaching the concentration v_2 corresponding to $\Delta G_{m_{iso}} = \Delta G_{m_{aniso}}$. The free energy of mixing of the isotropic mixture may be found from Eq. (2.1), if x is substituted for y. That of the nematic phase may be computed using Eq. (2.7). By equating these two equations and upon rearranging we end up with an expression of the form:

$$\frac{1}{v_2} = \frac{y}{2x} \left[\frac{2x}{y} + 2\ln(y/x) - y + x - 2\right] \qquad (2.17)$$

Simultaneous solution of Eq. (2.17) and Eq. (2.3), yields by trial-error calculation procedure $v_2 = 0.43545$ at $y = 5.10$ (for $x = 20$). Hence solving Eqs. (2.14) and (2.16) for v_2: 0 to 0.43545, will give the chemical potential curves of the solvent and solute respectively for isotropic mixture. To draw the anisotropic part, simultaneous solution of Eq. (2.13) and (2.3) will yield the solvent chemical potential. Similarly Eq. (2.15) and (2.3) will yield the chemical potential of the solute in nematic phase. The resulting curves are shown graphically in Fig. 2.2. As mentioned earlier all these calculations were carried out for athermal solutions; those for the non athermal will be explained later.
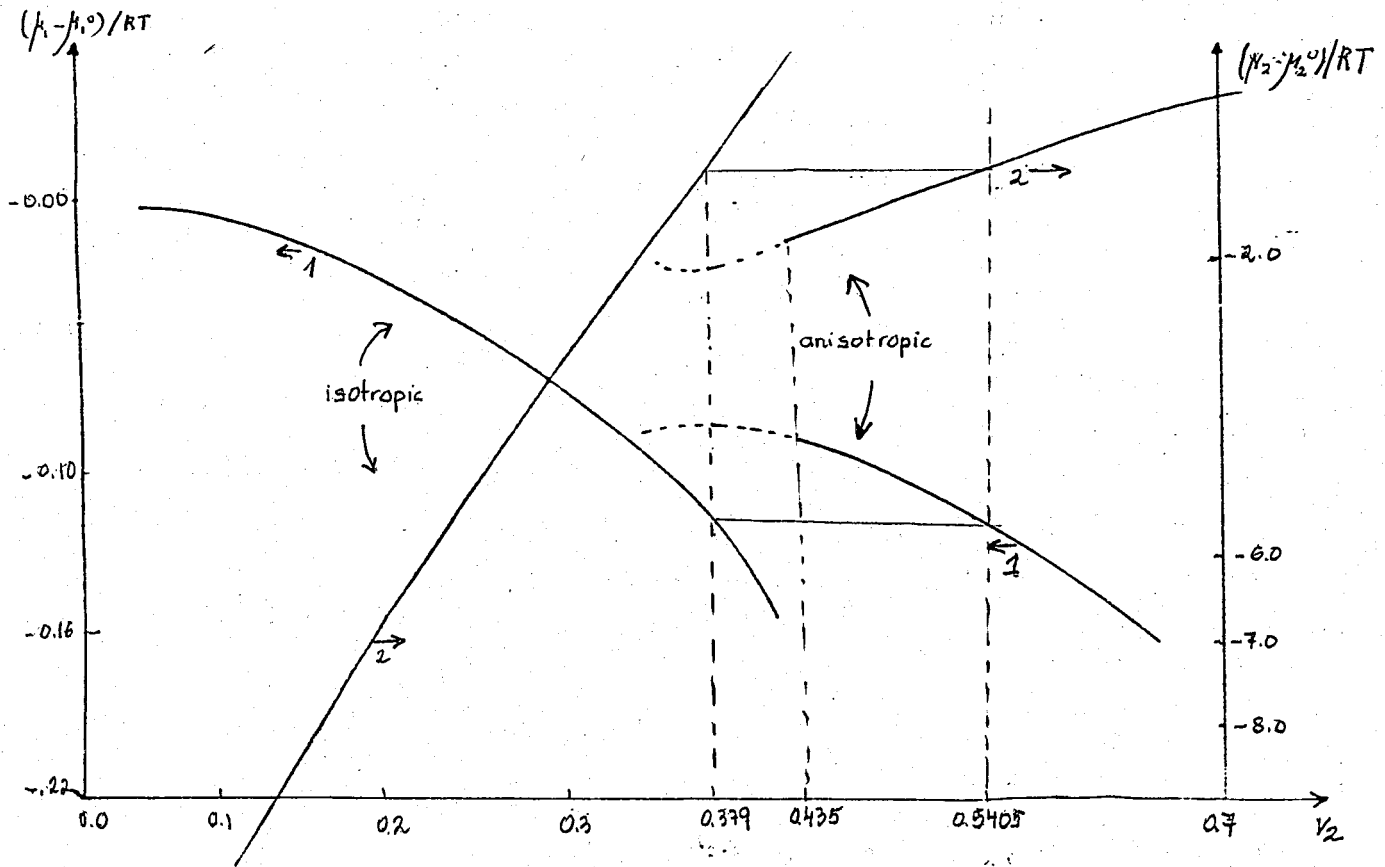
FIGURE 2.2 - Chemical potentials for the solvent and the solute for $\chi_1 = 0$, x = 20

2.3 PHASE EQUILIBRIUM IN SOLUTIONS

2.3.1 Athermal Solutions

For the coexistence of two liquid phases, the necessary and sufficient condition is that the chemical potential of either component, solvent or solute, must have the same numerical value in each phase. We may write the phase equilibrium condition as:

$$\mu_1 = \mu_1' \tag{2.18}$$

$$\mu_2 = \mu_2' \tag{2.19}$$

where accents are adopted to denote the more concentrated phase. Therefore we obtain, with the aid of Eqs. (2.13) and (2.16):

$$\ln(1 - v_2) + (1 - 1/x)v_2 + \chi_1 v_2^2 = \ln(1 - v_2') + (\frac{y - 1}{x})v_2'$$

$$+ \frac{2}{y} + \chi_1 v_2'^2 \text{ , for the solvent} \tag{2.20}$$

and

$$\ln(v_2/x) + (x - 1)v_2 - \ln x^2 + \chi_1 x(1 - v_2)^2 =$$

$$\tag{2.21}$$

$$\ln(v_2'/x) + (y - 1)v_2' - \ln y^2 + \chi_1 x(1 - v_2')^2 \text{, for the solute}$$

Numerical solutions of these equations, along with Eq. (2.3) will give the equilibrium concentrations in conjugated phases, the three unknowns being v_2, v_2' and y. Also, by a careful analysis of Fig. 2.2, for the chemical potentials of rodlike solutions with $x = 20$, one can see that at $v_2 = 0.379$ and $v_2' = 0.5405$, $\mu_1 = \mu_1'$ and $\mu_2 = \mu_2'$; hence these volume fractions are the equilibrium ones for $x = 20$.

2.3.2 Non Athermal Solutions

Even a small positive solvent-solute interaction parameter χ_1, has a marked effect on the course of μ_1 with v_2, as is illustrated in Fig. 2.3. The outstanding feature is the emergence of a maximum at a higher concentration. A similar behaviour is observed for $x = 20$, shown in Fig. 2.4.
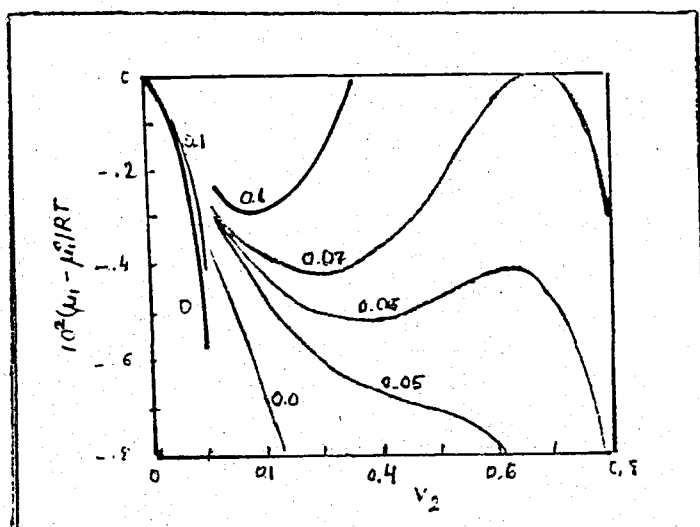
FIGURE 2.3 - Solvent chemical potentials for non athermal solution with $x = 100$

The presence of the maximum together with the preceeding minimum raises the possibility for coexistence of two anisotropic phases. Indeed, for $0.055 < \chi_1 < 0.08$ we have two conjugate nematic phases in equilibrium together with an isotropic-anisotropic pair, hence two heterogeneous regions: one involving an isotropic phase in equilibrium with a dilute nematic phase and the other, a pair of anisotropic phases. At $\chi_1 = 0.07$, a stable coexistence of three phases is observed. This explanations can be understood more easily in connection with Fig. 2.5.
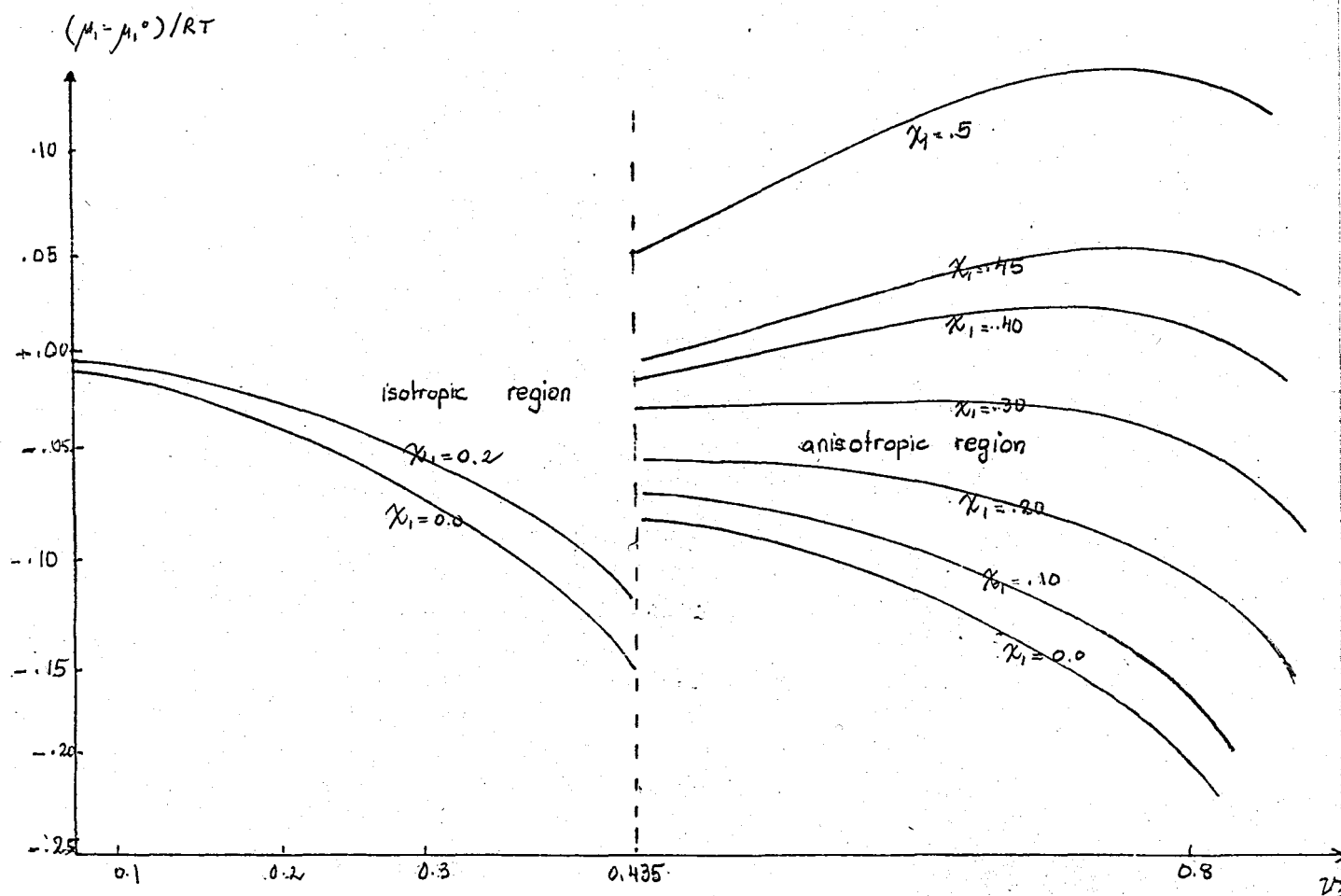
FIGURE 2.4 - Solvent chemical potentials for non athermal solutions with x = 20
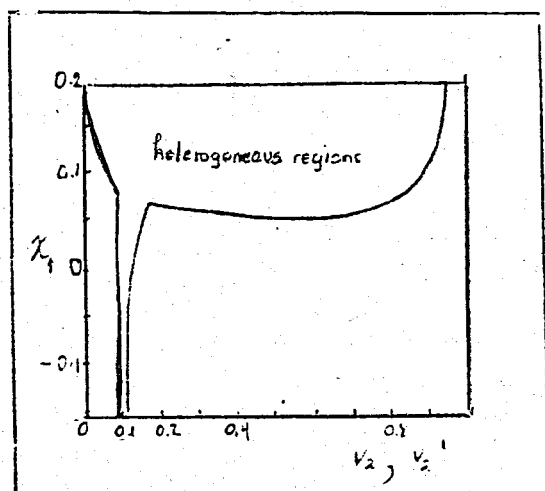
FIGURE 2.5 - Composition of phases in equilibrium for non athermal
rodlike solutions with x = 100

At χ_1 = 0.09 the composition of the concentrated phase reaches

v_2 = 0.873 where according to Eq. (2.3), y falls to unity. In order to

preserve consistency with the identification of y = 1, as the limit for

perfect orientation, we take y equal to unity for all χ_1 > 0.09, in cal-

culating the uppermost portions of Fig. 2.4. The equations for the phase

equilibrium, accordingly become (Flory, 1956):

$$\ln(1 - v_2) + (1 - 1/x) + \chi_1 v_2^2 = \ln[(1 - v_2') / (1 - v_2' + \frac{v_2'}{x})]$$

$$+ \chi_1 v_2'^2 \qquad (2.22)$$

$$\ln(v_2/x) + (x - 1)v_2 - \ln x^2 + \chi_1 x(1 - v_2)^2 =$$
$$\ln[(v_2'/x)/(1 - v_2' + v_2'/x)] + \chi_1 x(1 - v_2')^2 \qquad (2.23)$$

in which the solute chemical potentials for the dilute phase are equated to those of regular solution theory for the concentrated phase.

The sudden shift in the concentration v_2', from ~ 0.15 to > 0.9, brought above by a comparatively small change in χ_1 is of great importance. Also, these values of χ_1-parameter considered, are small compared to those commonly encountered in polymer-solvent systems. Calculations were done for $x = 20$, to obtain $\chi_1 = 0.4825$, for $y = 1$ (together with $v_2 = 0.155$) by simultaneous solution of Eq. (2.22) and Eq. (2.23), making use of $v_2' = 0.910$ (obtained from Eq. (2.3) for $y = 1$). Hence, for $x = 20$, above $\chi_1 = 0.4825$, the compositions of two conjugate phases were computed by solving Eq. (2.22) and Eq. (2.23), while for $\chi_1 < 0.4825$, Eq. (2.20) and (2.21) were used. The resulting curves are drawn in Fig. 2.4.

We are mostly interested in the region were a highly concentrated anisotropic phase is in equilibrium with a fairly dilute isotropic phase, due to the effect of a positive heat interaction parameter. This region corresponds to values of χ_1-parameter, obeying Eqs. (2.22) and (2.23), in general.

To summarize, phase separation arises spontaneously, in solutions of rigid rodlike particles, provided the macromolecular volume fraction exceeds a critical value v_2^*, this value decreasing as particle asymmetry increases (i.e. for higher x). Whereas both phases in equilibrium are predicted to be fairly dilute in the case of athermal systems, a comparatively small, positive energy interaction parameter χ_1, causes the concentration of the nematic phase to increase sharply. If the particles are of uniform structure even a smectic or cholesteric order can be observed in this concentrated phase, depending on the nature of the particles.

III. EFFECT OF HOMOGENEOUS FLOW ON
PHASE TRANSITION

Flory's theory of phase equilibria of rodlike molecules can be applied to a solution subject to homogeneous velocity field, by incorporating into the expression for the free energy of mixing, an additional term, accounting for the contribution of the flow. This additional term, as will be shown below, can be found easily, provided that the velocity field admits a potential so that we can speak of equilibrium condition of macromolecules, as already pointed out by Kramers (1946). Marucci and Ciferri (1975) analyzed phase equilibria in solutions exhibiting a nematic ordering under extensional flow. In this chapter, we will derive a most general formula, applicable not only to irrotational flows but to any type of homogeneous flow, by an appropriate selection of the reference frame.

3.1 MOTION OF THE POLYMER MOLECULE

A polymer molecule is idealized as a rigid rod CD, with center of mass A. $Oz_1z_2z_3$ is the laboratory fixed coordinate system. Let the molecule be composed of x segments and $\underset{\sim}{x}_i$ is the vector (subscript $\sim$ denotes vector) from the center of mass to the i'th segment located at B. Let us assume the polymer molecule is suspended in a liquid flowing with velocity $\underset{\sim}{v}'$. Then it will be set in motion by the frictional forces

acting upon each of the segments. The center of gravity A, will be moving with the velocity of the fluid at the position where this center is momentarily situated (neglecting the Brownian motion). This situation is referred to in the literature as "no drift condition" (Eringen, 1967).

Let r_A = distance from the origin to the center of mass A

r_B = distance from the origin to the point B

v_B' ≡ velocity of the fluid at B

v_B'' ≡ velocity of rod at B

v_B ≡ relative velocity at B = $v_B' - v_B''$ (3.1)

ω = instantaneous angular velocity.

We assume that ω coincides with the angular velocity of the fluid, at point A. This assumption is the rotational counterpart of the no drift condition stated above. From continuum theory the angular velocity for rigid rotation, is related to the vorticity tensor Ω of the fluid (subscript ≈ denotes the tensors). Then,

$$v_B'' = v_A'' + (\omega \times r_i)$$
$$= v_A' + (\tfrac{1}{2}\Omega \times r_i)$$
      (3.2)

combining Eqs. (3.1) and (3.2), we obtain,

$$v_B = (v_B' - v_A') - (\omega \times r_i)$$
      (3.3)

But for homogeneous flow,

$$v_B' - v_A' = v'(r_B) - v'(r_A) = v'(r_A - r_B) = v'(r_i)$$

Substituting this result in Eq. (3.3), we get:

$$v_B = v'(r_i) - (\omega \times r_i)$$
      (3.4)

Let $\underset{\sim}{F}_B$ denote the friction force acting on the rod, at point B. By definition $\underset{\sim}{F}_B = \xi \underset{\sim}{v}_B$ where ξ is the friction coefficient. Hence,

$$\underset{\sim}{F}_B = \xi(v'(\underset{\sim}{r}_i) - (\underset{\sim}{\omega} \times \underset{\sim}{r}_i))$$

Let $\underset{\sim}{M}_i$ denote the moment exerted by $\underset{\sim}{F}_B$ about a:

$$\underset{\sim}{M}_i = \underset{\sim}{r}_i \times \underset{\sim}{F}_B = \xi \underset{\sim}{r}_i \times [\underset{\sim}{v}'(\underset{\sim}{r}_i) - (\underset{\sim}{\omega} \times \underset{\sim}{r}_i)] \tag{3.5}$$

Now, let us consider the quantity in the brackets. This term represents the velocity of the fluid as observed from a reference frame rotating with an angular velocity ω. Hence it can be viewed as the fluid velocity without the rotational part; provided that the velocity is decomposed into two parts, the one rotational and the other irrotational. The term in brackets will stand for the irrotational part and will be the one responsible for the moment exerted on the rod. As a result it can be expressed in terms of a velocity potential $\phi(\underset{\sim}{r}_i)$ such that

$$[\underset{\sim}{v}'(\underset{\sim}{r}_i) - (\underset{\sim}{\omega} \times \underset{\sim}{r}_i)] = -\underset{\sim}{\nabla}\phi(\underset{\sim}{r}_i) \tag{3.6}$$

Consequently, the friction forces exerted by the liquid upon the rod admit a potential and the moment of these forces on the i'th segment B is given by

$$\underset{\sim}{M}_i = -\xi(\underset{\sim}{r}_i \times \underset{\sim}{\nabla}\phi(\underset{\sim}{r}_i)) \tag{3.7}$$

so that the overall moment for the entire rod, composed of x segments will be:

$$\underset{\sim}{M} = \sum_{i=1}^{x} \{-\xi(\underset{\sim}{r}_i \times \underset{\sim}{\nabla}\phi(\underset{\sim}{r}_i))\} \tag{3.8}$$

The potential energy associated with this moment will be denoted by U_{G^*}.

$$U_G^* \equiv \int_0^\psi \underset{\sim}{M} \cdot d\underset{\sim}{\psi}$$

$$= \xi \sum_{i=1}^{x} \{ \int_0^\psi (\underset{\sim}{r}_i \times \underset{\sim}{\nabla}\phi(\underset{\sim}{r}_i)) \cdot d\underset{\sim}{\psi} \} \qquad (3.9)$$

where ψ is the instantaneous angular deviation of the axis of the rod from the nematic director.

To get a simpler form from Eq. (3.9), let us consider the terms within the integration.

For a rotation around the z-axis

$$\underset{\sim}{r} \times \underset{\sim}{\nabla}\phi = \{ r \cos\psi \left.\frac{\partial\phi}{\partial y}\right|_x - r \sin\psi \left.\frac{\partial\phi}{\partial x}\right|_y \} \underset{\sim}{k}$$

$$= \{ r \cos\psi \left.\frac{\partial\phi}{\partial\psi}\right|_x \left.\frac{\partial\psi}{\partial y}\right|_x - r \sin\psi \left.\frac{\partial\phi}{\partial\psi}\right|_y \left.\frac{\partial\psi}{\partial x}\right|_y \} \underset{\sim}{k} \quad (3.10)$$

But $\quad x = r \cos\psi \qquad \dfrac{\partial\psi}{\partial x} = -\dfrac{1}{r \sin\psi} = -\dfrac{1}{y}$

$\quad\quad y = r \sin\psi$

$$\frac{\partial\psi}{\partial y} = \frac{1}{r \cos\psi} = \frac{1}{x}$$

Inserting the last two equalities into Eq. (3.10), we obtain:

$$(\underset{\sim}{r} \times \underset{\sim}{\nabla}\phi) = \{ \left.\frac{\partial\phi}{\partial\psi}\right|_x + \left.\frac{\partial\phi}{\partial\psi}\right|_y \} \underset{\sim}{k}$$

then $\quad (\underset{\sim}{r} \times \underset{\sim}{\nabla}\phi) \cdot d\underset{\sim}{\psi} = \dfrac{\partial\phi}{\partial\psi} d\psi$

and $\quad U_G^* = \sum_{i=1}^{x} \xi \int_0^\psi \dfrac{\partial\phi(\underset{\sim}{r}_i)}{\partial\psi} d\underset{\sim}{\psi}$

or $\quad U_G^* = 2\xi \sum_{i=1}^{x/2} [\phi(\underset{\sim}{r}_i)] \Big|_0^\psi \qquad (3.11)$

Equation (3.11) provides a rather easy method for calculating the change in energy associated with the effect of homogeneous flow, by simply finding the potential function corresponding to the irrotational part of the flow. As explained by Kramers (1946), the error introduced by selection of a rotating frame is negligible.

The problem reduces now, to the derivation of Φ of the irrotational part of any homogeneous flow.

A homogeneous flow is represented by (Eringen, 1967):

$$v = \underset{\approx}{k} \cdot \underset{\sim}{r} \qquad \text{(subscript} \approx \text{denotes tensor)}$$

where $\underset{\approx}{k}$ is the velocity gradient tensor, which is traceless for incompressible fluids. As to the velocity potential of irrotational flows is defined as (Bird, et.al, 1977):

$$\Phi = -\frac{1}{2}(\underset{\approx}{k}: \underset{\sim}{r}\,\underset{\sim}{r}) \qquad\qquad (3.12)$$

where : indicates the double dot product.

In the section that follows, the application of the above theoretical arguments to some homogeneous flows will be discussed. We will concentrate mainly on simple shear flow, the most widely encountered rotational flow after a brief consideration of irrotational flows such as steady potential flow and elongational (or extensional) flow.

3.2   APPLICATION OF THE THEORY ESTABLISHED IN SECTION 3.1
       TO HOMOGENEOUS FLOWS

3.2.1 Irrotational Flows

Irrotational flow is characterized by the property (Slattery, 1972):

$$\underset{\approx}{\Omega} \equiv \text{vorticity tensor} = 0$$

i) Steady homogeneous potential flow is defined by $v = -\nabla \phi$ with $\phi = \frac{1}{2}(k:r\,r)$, in compact notation with δ_i, δ_j and δ_k representing the unit vectors in z_1, z_2 and z_3 directions we have

$$\phi = -\frac{1}{2}\{k_{ij}\,\delta_i\delta_j:(r_k\,\delta_k r_\ell \delta_\ell)\} \quad , \text{ in indicial notation}$$

$$= -\frac{1}{2}\{k_{ij}r_k r_\ell\,(\delta_i\delta_j:\delta_k\delta_\ell)\}$$

$$= -\frac{1}{2}\sum_{i=1}^{3}\sum_{j=1}^{3} k_{ij}r_i r_j$$

so that $\quad v_i = \partial[-\frac{1}{2}\sum_i\sum_j k_{ij}r_i r_j]/\partial r_i \quad\quad i = 1,2,3$

For potential flows we may write:

$$\dot{\gamma} \equiv \text{rate of deformation tensor} \equiv \nabla v + \nabla v^T = \sum_i\sum_j(\phi_{,ij} + \phi_{,ji})\delta_i\delta_j$$

and $\quad \Omega \equiv \nabla v - \nabla v^T = \sum_i\sum_j(\phi_{,ij} - \phi_{,ji})\delta_i\delta_j = 0$

where $\phi_{,ij}$ denotes the second order derivative of ϕ with respect to z_i then z_j.

For steady potential flow, Eq. (3.11) is directly applicable, for one molecule. As mentioned earlier, this term represents the contribution of the velocity field to ΔG_m, so that the whole expression for the free energy change of mixing becomes, by adding Eq. (3.11) to Eq. (2.1):

$$\frac{\Delta G_m}{kT} = n_1 \ln v_1 + n_2 \ln v_2 - (n_1 + yn_2)\ln[1 - v_2(1 - y/x)]$$

$$- n_2[\ln xy^2 - y + 1] + \chi_1 x\,n_2 v_1 + \xi\langle\sum_{i=1}^{x} \phi(r_i)\rangle \frac{n_2}{kT}$$

where average potential function over the n_2 macromolecules is to be considered.

ii) Extensional (or elongational) flow is identified by:

$$\underset{\approx}{k} = \begin{pmatrix} -\tfrac{1}{2}\Gamma & 0 & 0 \\ 0 & -\tfrac{1}{2}\Gamma & 0 \\ 0 & 0 & \Gamma \end{pmatrix}$$

so that

$$v_1 = -\frac{\Gamma}{2} z_1$$

$$v_2 = -\frac{\Gamma}{2} z_2$$

$$v_3 = \Gamma z_3$$

and

$$\Phi = -\frac{1}{2}[\underset{\approx}{k} : \underset{\sim}{r}\, \underset{\sim}{r}] = \frac{\Gamma}{4}[z_1^2 + z_2^2 - 2z_3^2]$$

or

$$= \frac{\Gamma}{2}[\frac{r^2}{2} - z^2] \qquad \text{in cylindrical coordinate.}$$

Application of Eq. (3.11) yields,

$$U_G^* = 2\xi \sum_i [\frac{\Gamma}{2}(\frac{r_i^2}{2} - z_i^2)]_0^\psi \tag{3.13}$$

Let

b = length of a segment

x_i = number of segments from the center of gravity to the

i'th segment (the total number of segments equals x).

In elongational flow the nematic director coincides with the direction of the flow. Hence ψ will represent the angle between the instantaneous position of the rod and the z-axis. Then r_i and z_i can be written in terms of ψ, b and x_i such that:

$$r_i = b\, x_i\, \sin\psi$$

$$z_i = b\, x_i\, \cos\psi$$

Substituting the above relationships in Eq. (3.13), we obtain:

$$U = 2\xi \frac{\Gamma}{2} \sum_{x_i=i}^{x/2} \left[\frac{b^2 x_i^2 \sin^2\psi}{2} - b^2 x_i^2 \cos^2\psi \right]_0^\psi \qquad (3.14)$$

$$= \Gamma\xi b^2 \sum_{x_i=i}^{x/2} x_i^2 \left[-1 + 3/2 \sin^2\psi \right]_0^\psi \qquad (3.15)$$

But

$$\sum_{x_i=0}^{x/2} x_i^2 = \left(\frac{x}{2}\right)\left(\frac{x}{2} + 1\right)(x + 1)/6 = \left(\frac{x^3}{24} + \ldots\ldots\right) \qquad (3.16)$$

Combining Eqs. (3.16) and (3.15), we end up with:

$$U_G^* \approx \frac{1}{16} \xi\Gamma b^2 x^3\sin^2\psi \qquad (3.17)$$

This expression is exactly the same as the one derived by Marucci (1975), though we reached the same conclusion by making use of Eq. (3.11). Marucci and Ciferri's approach, which is valid for elongational flow only, is based on the formulation of an expression for the moment of friction force exerted on the rod, while our method, provides a more powerful tool to deal with any type of homogeneous flow (even rotational) as will be shown below.

Equation (3.17) gives the potential energy associated with a single macromolecule, oriented such that its axis makes an angle ψ with the nematic director. For a system of n_2 macromolecules, randomly oriented, an average expression accounting for the most probable orientation should be used. In other terms, an expression for $\langle \sin^2\psi \rangle$ should be found. It is explained in Appendix A2, that

$$\langle \sin^2\psi \rangle = (y/x)^2 \qquad (3.18)$$

for random distribution. Inserting this last equality in Eq. (3.17) and

combining with Eq. (2.1), the full expression for the free energy becomes:

$$\frac{\Delta G_m}{kT} = n_1 \ln v_1 + n_2 \ln v_2 - (n_1 + yn_2)\ln[1 - v_2(1 - y/x)]$$

$$- n_2[\ln xy^2 - y + 1] + \chi_1 x \, n_2 v_1 + \frac{1}{2} G^* n_2 xy^2 \qquad (3.19)$$

where $G^* \equiv \frac{1}{8} \frac{\Gamma b^2}{kT/\xi}$, is a dimensionless quantity reflecting the ratio of the effect of the bulk flow to that of diffusional flow, the denominator (kt/ξ) defining the diffusion coefficient of the macromolecule (Villars, Benedek, 1974).

3.2.2 Rotational Flows

A motion in which the vorticity vector field does not vanish is said to be rotational. The vorticity vector field $\underset{\sim}{x}$, is defined as (Slattery, 1972):

$$\underset{\sim}{\Omega} = \underset{\sim}{\varepsilon} : \underset{\approx}{\Omega} = \varepsilon_{ijk} \, \Omega_{kj} \underset{\sim}{\delta}_i$$

$$= \frac{1}{2} \varepsilon_{ijk} \left(\frac{\partial v_k}{\partial z_j} - \frac{\partial v_j}{\partial z_k}\right)\underset{\sim}{\delta}_i \equiv \underset{\sim}{\nabla} \times \underset{\sim}{v}$$

where ε_{ijk} is the permutation symbol.

A rotational flow can be viewed as the superposition of two flows, one of them irrotational and the other being a uniform rotation. The effect of rotation can be neglected, if $\underset{\approx}{k}$, the velocity gradient tensor is not too large, as already explained. Then, the effect of flow can be described by the potential function associated with the irrotational part of our rotational velocity field. Hence our first task is to divide the flow into two parts. A practical method will be to extract the irrotational part by making use of Eq. (3.4). The next step will be to evaluate the function ϕ corresponding to this irrotational flow and then to incorporate

this potential function within the most general expression for ΔG_m; also, the flow induced energy term must be averaged over the ensemble of n_2 macromolecules, by considering their instantaneous angular displacement from the nematic director, whose direction is prescribed by the type of flow in question.

These explanations will be made clearer, in connection with the example of simple shear flow, the simplest and most common type of rotational flow. In a volume element of sufficiently small size, the well-known Poiseuille flow, may be approximated by simple shear flow (Kramers, 1946). The components of the simple shear flow in cartesian coordinate are

$$v_1 = \Gamma z_2 \quad \text{where } \Gamma \text{ is a constant (velocity gradient)}$$
$$v_2 = 0 \tag{3.20}$$
$$v_3 = 0$$

Then
$$\underset{\sim}{\Omega} = \epsilon_{ijk} \{\frac{1}{2} \underset{\sim\sim}{\nabla v} - \underset{\sim\sim}{\nabla v}^T\} = \frac{1}{2} \begin{pmatrix} 0 \\ 0 \\ -2\Gamma \end{pmatrix}$$

From continuum mechanics (Eringen, 1967), the angular velocity $\underset{\sim}{\omega}$ for rigid rotation in shear flow, equals one half of the vorticity vector. Hence

$$\underset{\sim}{\omega} = \underset{\sim}{\Omega}/2 = [0 \quad 0 \quad -\Gamma/2]^T$$

With these informations, we may apply Eq. (3.4) to find out the irrotational part of the flow, i.e.,

$$\underset{\sim}{v} = \underset{\sim}{v}' - (\underset{\sim}{\omega} \times \underset{\sim}{r}) = \begin{pmatrix} \Gamma z_2 \\ 0 \\ 0 \end{pmatrix} - \begin{pmatrix} 0 \\ 0 \\ -\Gamma/2 \end{pmatrix} \times \begin{pmatrix} z_1 \\ z_2 \\ z_3 \end{pmatrix}$$
$$= (\Gamma z_2 \quad 0 \quad 0)^T - (\frac{\Gamma}{2}z_2 \quad \frac{\Gamma}{2}z_1 \quad 0)^T = (\frac{\Gamma}{2}z_2 \quad \frac{\Gamma}{2}z_1 \quad 0)^T \tag{3.21}$$

Superposing to the irrotational flow given by Eq. (3.21), a uniform rotation we must end up with Eq. (3.20). Clearly this rotational velocity field will be given by:

$$v_1 = \frac{1}{2}\Gamma z_2$$

$$v_2 = -\frac{1}{2}\Gamma z_1 \qquad\qquad (3.22)$$

$$v_3 = 0$$

Now, our objective is to find the potential function associated with the irrotational flow given by Eq. (3.21). Clearly, this will be done by making use of Eq. (3.21); First $\underset{\approx}{k}$ has to be determined

$$\underset{\sim}{v} = \underset{\approx}{k} \cdot \underset{\sim}{r} = \begin{bmatrix} k_{11} & k_{12} & k_{13} \\ k_{21} & k_{22} & k_{23} \\ k_{31} & k_{32} & k_{33} \end{bmatrix} \cdot \begin{bmatrix} z_1 \\ z_2 \\ z_3 \end{bmatrix} = \begin{bmatrix} k_{11}z_1 + k_{12}z_2 + k_{13}z_3 \\ k_{21}z_1 + k_{22}z_2 + k_{23}z_3 \\ k_{31}z_1 + k_{32}z_2 + k_{33}z_3 \end{bmatrix}$$

but

$$\underset{\sim}{v} = \begin{bmatrix} (1/2)\Gamma z_2 \\ (1/2)\Gamma z_1 \\ 0 \end{bmatrix} \qquad\qquad (3.23)$$

Comparison of the two equations above, yields

$$\underset{\approx}{k} = \begin{bmatrix} 0 & \Gamma/2 & 0 \\ \Gamma/2 & 0 & 0 \\ 0 & 0 & 0 \end{bmatrix}$$

but

$$\underset{\sim}{r}\,\underset{\sim}{r} = \begin{bmatrix} z_1^2 & z_1 z_2 & z_1 z_3 \\ z_1 z_2 & z_2^2 & z_2 z_3 \\ z_3 z_1 & z_3 z_2 & z_3^2 \end{bmatrix}$$

so that $\quad \Phi = -\frac{1}{2} \underset{\approx}{k} : \underset{\sim}{r} \, \underset{\sim}{r} = -\frac{1}{2}[\Gamma z_1 z_2 + \frac{1}{2} \Gamma z_1 z_2]$

Finally

$$\Phi = -\frac{1}{2} \Gamma z_1 z_2 \tag{3.24}$$

Using the potential formalism given by Eq. (3.11), we obtain, for the contribution of the flow to ΔG_m,

$$U_G = 2\xi \sum_{i=1}^{x/2} [-\frac{1}{2} \Gamma z_1 z_2]_i \Big|_o^\psi \quad, \text{ per macromolecule} \tag{3.25}$$

To find a more convenient expression for the flow-induced energy term, we have to investigate the direction of the nematic director. The formal procedure to find out this direction for any type of flow, is explained in Appendix A3. For the simple case of simpe shear flow, Fig. 3.1, will help to visualize the situation.
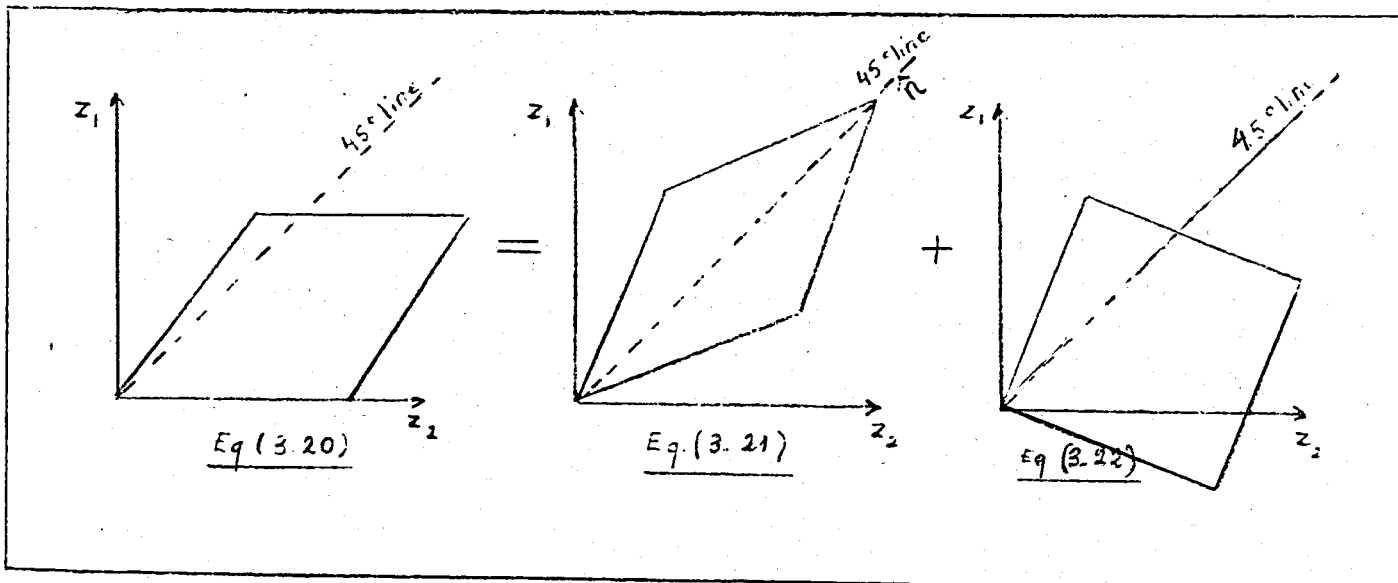
FIGURE 3.1 - Schematic representation of a fluid body under shear flow

As can be seen clearly, the effect of the irrotational part is analogous to that of an elongational the only difference residing in the shifting of the nematic director by an angle of 45°. Hence, in this present case, for the i'th segment of the rodlike molecule, the Eq. (3.26) will hold

$$(z_1)_i = b \, x_i \, \cos(\psi + 45^O)$$
$$(z_2)_i = b \, x_i \, \sin(\psi + 45^O)$$

(3.26)

Inserting these relationships in Eq. (3.25), and summing over all segments, we obtain, the flow induced change in energy per molecules, as follows

$$U_G{}^* = 2\xi \sum_{i=1}^{x/2} [- \frac{1}{2} \Gamma b^2 x_i^2 \cos(\psi+45)\sin(\psi+45)]$$

but

$$\cos(\psi+45)\sin(\psi+45) = (\cos\psi \, \cos45 - \sin\psi \, \sin45)(\cos\psi \, \sin45 + \cos\psi \, \sin$$
$$= [\sqrt{2}/2]^2[\cos^2\psi - \sin^2\psi]$$

Back substituting this relationship in Eq. (3.27),

$$U_G{}^* = -2\xi\Gamma b^2 \sum_{i=1}^{x/2} [\frac{x_i^2}{2}(\cos^2\psi - \sin^2\psi)]_0^\psi$$

$$U_G{}^* = - \Gamma b^2 \xi \sum_{i=1}^{x/2} x_i^2[-2\sin^2\psi]$$

(3.27)

For a system consisting of n_2 macromolecules, with random spatial orientation, the total energy contribution to ΔG_m, will be given by

$$U_G{}^* = n_2(x^3/24)\Gamma\xi \, b^2 <\sin^2\psi>$$

(3.28)

where Eq. (3.16) is inserted in Eq. (3.27).

It was previously stated that $<\sin^2\psi> \approx (y/x)^2$

then

$$\frac{U_G^*}{kT} = \frac{1}{2} G^* n_2 x y^2 \qquad (3.29)$$

where $\qquad G^* \equiv \frac{1}{12} \frac{\Gamma b^2}{kT/\xi} \qquad (3.30)$

As expected, an expression similar to that of elongational flow is obtained, differing only by a proportionality constant. Hence, Eq. (3.19) is valid for simple shear flow, provided that G^* is defined by Eq. (3.30).

3.3 EXTENSION OF FLORY's THEORY OF PHASE EQUILIBRIA FOR QUIESCENT SOLUTION TO THAT SUBJECT TO HOMOGENEOUS FLOW

Once an expression for the free energy of mixing is obtained, the relative effect of the flow field can be deduced from the equation relating the equilibrium compositions in the nematic phase, to their orientation parameter. This equation, analogous of Eq. (2.3), is again derived by differentiating ΔG_m (of Eq. 3.19) with respect to y and equating to zero, to get:

$$v_2' = \frac{x}{x - y} [1 - \exp\{-\frac{2}{y} + G^* x y\}] \qquad (3.31)$$

As explained in Chapter 2, the above equation gives the set of (v_2', y), that minimizes ΔG_m. It can easily be noticed that the volume fraction of the polymer in nematic phase v_2', will be equal to zero, at

$$G^*_{critical} = \frac{2}{x^3} \qquad (3.32)$$

Hence, for values of G^* higher than this critical value no phase separation occurs; the solution is totally anisotropic. As to values $G^* < G^*_{critical}$, either totally isotropic or two phase system can be observed depending on macromolecular volume fraction. It has been checked (Marucci, Ciferri, 1975) that the net effect of the flow field is the shifting of the phase separation interval towards smaller values of v_2.

The equilibrium volume fractions in the two phases are calculated by equating the chemical potentials of each component, separately in the two phases. The chemical potentials of the solvent μ_1, and the solute μ_2, under anisotropic conditions are given by:

$$\frac{\mu_1 - \mu_1^0}{RT} = \ln(1 - v_2') + \frac{y - 1}{x} v_2' + \frac{2}{y} + \chi_1 x v_2'^2 - G^* xy \qquad (3.33)$$

$$\frac{\mu_2 - \mu_2^0}{RT} = \ln(v_2'/x) + (y - 1)v_2 + 2 - \ln y^2 + \chi_1 x(1 - v_2)^2$$

$$- \frac{1}{2} G^* xy \qquad (3.34)$$

For the isotropic solution

$$\frac{\mu_1 - \mu_1^0}{RT}\bigg|_{y=x} = \ln(1 - v_2) + (1 - \frac{1}{x})v_2 + \chi_1 v_2^2 \qquad (3.35)$$

$$\frac{\mu_2 - \mu_2^0}{RT}\bigg|_{y=x} = \ln(v_2/x) + (x - 1)v_2 - \ln x^2 + \chi_1 x(1 - v_2)^2$$

$$+ \frac{G^* x^3}{2} \qquad (3.36)$$

Equating Eq. (3.33) to Eq. (3.35) and Eq. (3.34) to Eq. (3.36) and considering Eq. (3.31) too, we will have three equations, whose simultaneous solutions will yield the three unknowns v_2, v_2' and y.

A few representative results, calculated by Marucci and Ciferri (1975), for athermal solutions under extensional flow are shown in Fig. 3.2. Obviously, the same graph will be valid for simple shear flow too, provided that G^* is defined by Eq. (3.30).
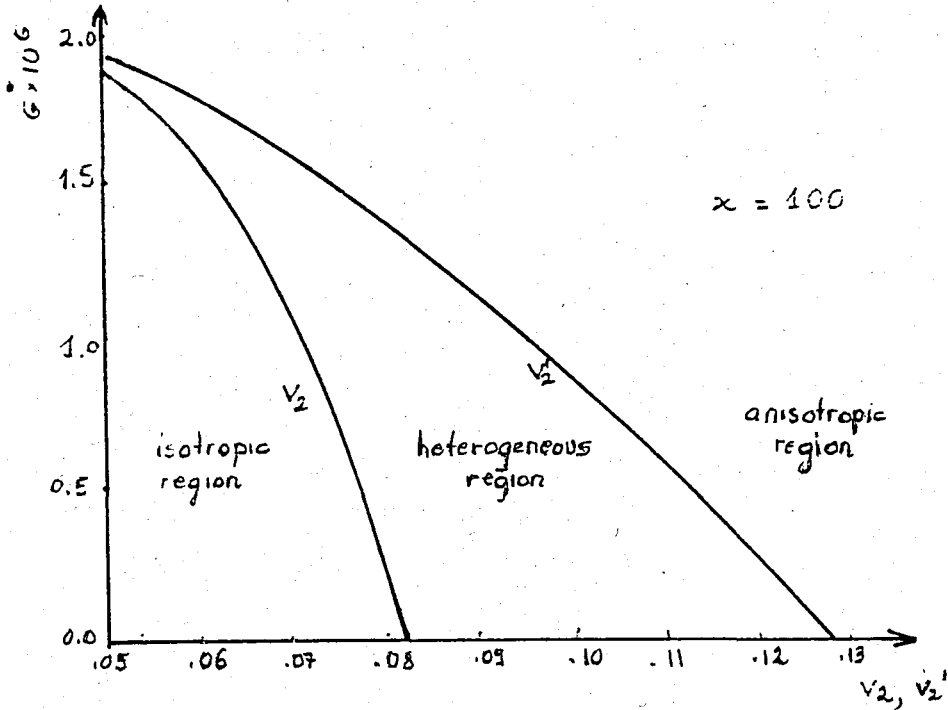
FIGURE 3.2 - Equilibrium concentrations in the two phases versus G^*

IV. CONTRIBUTION OF STRESS-INDUCED DIFFUSION TO PHASE EQUILIBRIUM

In the preceeding chapter, the role of the fluid mechanics in the process of nematic phase formation in dilute solutions of rodlike particles has been analyzed, concentrating mostly on elongational and shear flows. Recently, it has been recognized (Tirrell, et.al, 1977) that the well-known thermodynamic driving force, entropic in nature, which tends to restore the molecules to their unperturbed dimensions, will cause the macromolecules to diffuse from regions of higher stress, to regions or lower stress, if such regions are present, resulting in a non uniform spatial distribution of macromolecular concentration.

4.1 THEORY OF STRESS INDUCED DIFFUSION

Let us consider a solvent-solute system, with initial concentration spatially uniform. The application of a stress field which is not constant over the domain occupied by the mixture, will produce a thermodynamic driving force for the diffusion of the solute towards regions of lower stress. We may express this force as the gradient of a potential field, say V, such that

$$\underset{\sim}{F} = -\underset{\sim}{\nabla}V \qquad (4.1)$$

On the other hand

$$F = \xi v = v/B \tag{4.2}$$

where B is defined to be the mobility and equals D/kT, where D is the diffusion coefficient.

Eqs. (4.1) and (4.2), yield

$$v = -B\nabla V = \frac{D}{kT}\nabla V \tag{4.3}$$

This force gives rise to a stress-induced molar flux, J_s, of the polymer molecules. Let $\bar{c}$ denote the local solute molar concentration in moles/volume. Then by definition, (Silebi, McHugh, 1979):

$$J_s = \bar{c}\, v \tag{4.4}$$

Combining Eqs. (4.3) and (4.4), we obtain

$$J_s = -\frac{D\bar{c}}{kT}\nabla V \tag{4.5}$$

This stress induced flux will produce a concentration gradient which, in turn will produce a flux, J_F, due to Fickian diffusion, such that

$$J_F = -D\,\nabla\bar{c} \tag{4.6}$$

Then, the net flux in the system, will be

$$J = J_s + J_F = -D[\nabla\bar{c} + \frac{\bar{c}}{kT}\nabla V] \tag{4.7}$$

At equilibrium, the net flux will be zero; then assuming cylindrical symmetry, for a flow in the z-direction, Eq. (4.7) gives:

$$\frac{d\bar{c}}{dr} + \frac{\bar{c}}{kT} \frac{dV}{dr} = 0 \qquad (4.8)$$

or

$$\frac{d\bar{c}}{c} = - \int \frac{dV}{kT}$$

$$\bar{c} = A' \exp\{- \frac{\Delta V}{kT}\}$$

where A' is a constant. Upon rearrangement, we may write:

$$\frac{\Delta V}{kT} + \ln \bar{c} = \ln A' = \text{constant} \qquad (4.9)$$

But

$$\bar{c} = \frac{\text{moles of solute}}{\text{total volume}} = \frac{\text{moles of solute}}{\text{volume of solute}} \times \frac{\text{volume of solute}}{\text{total volume}}$$

or

$$c = \frac{1}{V_m} v_2 \qquad (4.10)$$

where V_m is the molar volume of the solute, then

$$\ln \bar{c} = \ln v_2 - \ln V_m \qquad (4.11)$$

Substituting Eq. (4.11) in Eq. (4.9), we obtain,

$$\frac{\Delta V}{kT} + \ln v_2 = \ln V_m + \ln A' = \text{constant} \qquad (4.12)$$

In our system of rodlike particles in solution, under homogeneous flow,

$$\Delta V \equiv \frac{\Delta G_m}{n_2} \; , \; \text{given by Eq. (3.19).}$$

Hence, for any region i

$$[\frac{\Delta G_m}{n_2 kT} + \ln v_2]_i = \text{constant} \qquad (4.13)$$

4.2 EFFECT OF DIFFUSION ON A SYSTEM OF RODLIKE PARTICLES UNDER POISEUILLE FLOW

Now, let us confine our attention to a system of rodlike particles under Poiseuille flow, in a narrow cylindrical pipe. The flow near the wall can be approximated by simple shear flow, if a very small region is considered. Hence in this region Eq. (3.19), together with Eq. (3.31) will describe the change in free energy.

If we investigate flow near surfaces, we observe the drag caused completely by viscous shear forces associated with the variation of velocity from zero at the solid surface, to $\underline{v}$ in the undisturbed stream This region near a solid, where the fluid motion is affected by the solid boundary is called the boundary layer. Within this region, the layers of fluid near the surface are retarded by viscous friction or unfavourable pressure gradient, in the presence of surface roughnesses. These two factors are enough to cause the fluid near the surface to come to rest and even to flow in the reverse direction (Bennett, Myers, 1962), as shown in Fig. 4.1.
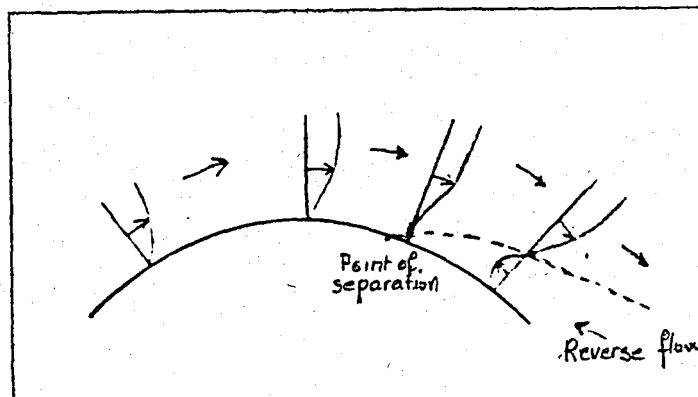
FIGURE 4.1 - Separation in flow, past a solid surface

The boundary layer, then leaves the surface. This phenomenon, called separation is more frequent with laminar flows (Evans, 1968).

On the basis of the above explanations, it is a good assumption to accept the fluid in a thin region (denoted by subscript B), next to the boundaries of our conduit, as stationary. Also, let us denote by subscript A, the region near the walls, where the Poiseuille flow is approximated by simple shear flow. Following, the theory of stress induced diffusion, the particles in region A, will tend to diffuse towards region B. Since the velocity gradient is flat in the center of the tube and steeper near the wall, there will be a slight diffusion towards the center of conduit, too. However, as far as we are concerned, we will consider only the boundaries where the stress induced diffusion is relatively intensified.

For a sufficiently dilute solution, the solute molecules in region A, will be distributed isotropically. As to the stagnant region B, depending on the solute volume fraction isotropic, nematic or both phases can be observed, according to Flory's theory of phase equilibria for quiescent solutions.

Assume both phases are isotropic. Then substitution of Eq. (3.19) in Eq. (4.13), gives:

$$\frac{1}{n_{2A}} [n_{1A}\ln V_{1A} + n_{2A}\ln v_{2A} - n_{2A}\ln x^3 - x + 1] + \chi_1 x\, n_{2A}v_{1A}$$

$$+ \frac{1}{2} G^* n_{2A}x^3] + \ln v_{2A} = \frac{1}{n_{2B}}[n_{1B}\ln v_{1B} + n_{2B}\ln v_{2B}$$

$$- n_{2B}(\ln x^3 - x + 1) + \chi_1 x\, n_{2B}v_{1B}] + \ln v_{2B}$$

or

$$\frac{n_{1A}}{n_{2A}} \ln v_{1A} + 2\ln v_{2A} - \chi_1 x\, v_{1A} + \frac{1}{2} G^* x^3 =$$

$$\frac{n_{1B}}{n_{2B}} \ln v_{1B} + 2\ln v_{2B} + \chi_1 x\, v_{1B} \qquad (4.14)$$

But

$$\frac{n_{1A}}{n_{2A}} = \frac{x\, v_{1A}}{v_{2A}} = \frac{x(1 - v_{2A})}{v_{2A}}$$

$$\qquad\qquad\qquad\qquad (4.15)$$

$$\frac{n_{1B}}{n_{2B}} = \frac{x(1 - v_{2B})}{v_{2B}}$$

Inserting Eq. (4.15) in Eq. (4.14), we obtain,

$$\frac{1}{2} G^* x^3 + \frac{x}{v_{2A}}(1 - v_{2A})\ln(1 - v_{2A}) + 2\ln v_{2A} + \chi_1 x(1 - v_{2A}) =$$

$$\frac{(1 - v_{2B})}{v_{2B}} x \ln(1 - v_{2B}) + 2\ln v_{2B} + \chi_1 x(1 - v_{2B}) \qquad (4.16)$$

As can be seen from Eq. (4.16), the contribution of the flow field to the free energy is counterbalanced by the decrease in volume fraction of macromolecules, so that a diffusion towards stagnant region takes place.

The concentration gradient between the two regions is higher as the velocity increases or consequently for higher G^* values. However, the increase in G^* beyond $G^*_{critical}$, will induce anisotropy to the previously disordered flowing system. So Eq. (4.16) is no longer valid and should be replaced by an appropriate expression relating the free energy of the stagnant isotropic fluid to that of the flowing fluid

exhibiting nematic ordering. Consequently, the diffusion in this case will be governed by the following expression, whose derivation is quite similar to that of Eq. (4.16):

$$\frac{x}{v_{2A}}(1 - v_{2A})\ln(1 - v_{2A}) + 2\ln v_{2A} - \frac{x}{v_{2A}}(1 - v_{2A} + y\frac{v_{2A}}{x})$$

$$[\ln(1 - v_{2A} + y\frac{v_{2A}}{x})] + \chi_1 x(1 - v_{2A}) + \frac{1}{2}G^* xy^2 - [\ln[xy^2] - y + 1]$$

$$= \frac{x}{v_{2B}}(1 - v_{2B})\ln(1 - v_{2B}) + 2\ln v_{2B} + \chi_1 x(1 - v_{2B})$$

$$- [\ln x^3 - x + 1] = 0 \qquad\qquad (4.17)$$

Eq. (4.17), combined with Eq. (3.31) will describe the behaviour of macromolecules in homogeneous flow. By making use of these equations, one can determine the solute concentration at the wall, for a given system. Calculations will show that the amount of accumulation increases with increasing flow rate, but is more strongly dependent on χ_1-parameter.

To be able to visualize the behaviour of macromolecules under these conditions, and to determine the parameters that prescribe this behaviour, it is useful to examine more closely a solvent-solute system with known solute fraction, say 0.01, and study the effect of variables such as flow rate, axis ratio x, solvent-solute interaction parameter χ_1, on the amount of accumulation by stress-induced diffusion, on stationary locations.

4.3   CALCULATIONS

As a first approach, let us consider the influence of the increase in flow rate to the amount of change in macromolecular concentration, for athermal system.

An increase in the dimensionless quantity G^* is equivalent to either an increase in the flow rate (or the velocity gradient $\underset{\approx}{k}$) or a decrease in the diffusivity coefficient (which is proportional to temperature and inversely proportional to friction coefficient). As expected, as G^* increases, the stress-induced diffusion being intensified, the concentration of the macromolecules in stationary regions increases too. The corresponding curve is shown in Fig. 4.2 (for $\chi_1 = 0$). Fig. 4.2 was constructed for rodlike particles of axis ratio equal to 100, having a volume fraction of 0.01 in the flowing stream. As can be seen from the graph, increase in G^* causes the solute concentration in the quiescent solution (v_{2B}), to reach levels of about five times that of the flowing stream. The procedure to obtain these curves is based on a trial-error method consisting of first evaluating the disorientation parameter y from Eq. (3.31) and then using Eq. (4.17) to compute v_{2B} by iterative calculations, for given χ_1 and G^* values, keeping $x = 100$ fixed.

For non athermal systems, the relative effect of the energy interaction parameter χ_1, becomes more conspicious as the flow rate increases (or as an alternative for compounds with relatively lower diffusion coefficients).

Now, before proceeding to search for the possibility of a concentrated nematic phase at the stagnant regions, it is instructory to revise briefly the phase transition in non athermal quiescent solutions, with particles of $x = 20, 50, 100$, for comparison. We will concentrate mainly on the uppermost portion of the plotting showing the equilibrium compositions of the two phases. We will start with the one for $x = 100$ (See Fig. 2.4). As mentioned earlier, above $\chi_1 = 0.09$, the identification of $y = 1$ as the limit for perfect orientation requires the use of chemical potential expressions for regular solutions; the equations of
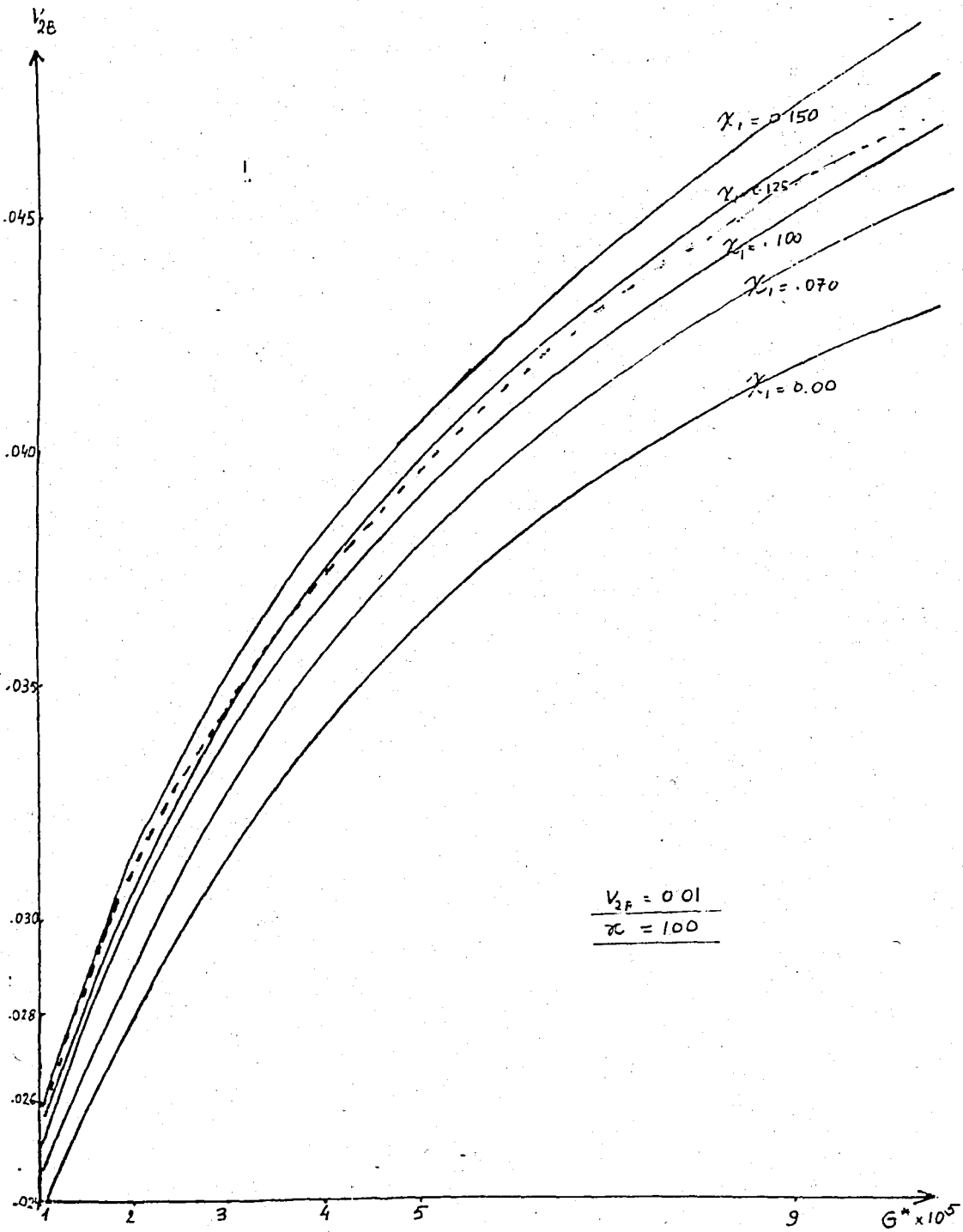
FIGURE 4.2 - Variation of solute volume fraction in the stagnant region with G^*

phase   equilibrium, accordingly, will be (2.22) and (2.23). Simulta-
neous solution of these two equations, by iterative trial and error pro-
cedure gives. Fig. 4.3, which is nothing else than the uppermost portion
of Fig. 2.45. As can be seen a very concentrated nematic phase coexists
with the isotropic phase.

Similar calculations were done for solutions with x = 20 and
x = 50. For x = 2, it was already calculated, in Chapter 2, that Eqs.
(2.22) and (2.23) were valid starting from x_1 = 0.4825 corresponding to
the point where y, the disorientation parameter becomes equal to unity.
So calculations were carried out for x_1 > 0.4825. Same reasoning was
used for x = 50 too. The resulting curves are shown in Fig. 4.4. The
compositions of the anisotropic phase are not shown in the graph; they
are tabulated below.

x = 20			x = 50			x = 100		
x_1	v_{2B}	v'_{2B}	x_1	v_{2B}	v'_{2B}	x_1	v_{2B}	v'_{2B}
0.4826	0.155	0.9100	0.20	0.0825	0.9003	0.10	0.054	0.895
0.550	0.062	0.92345	0.23	0.0557	0.01478	0.11	0.0459	0.9054
0.600	0.024	0.93207	0.25	0.0380	0.92265	0.125	0.0336	0.9180
0.650	0.0089	0.93943	0.28	0.0169	0.93247	0.135	0.0255	0.9248
0.700	0.00335	0.94568	0.30	0.0080	0.93979	0.145	0.0180	0.9306
						0.150	0.0144	0.9335
						0.155	0.0115	0.9357

FIGURE 4.3 - Phase diagram for x = 100, χ_1 > 0.1

FIGURE 4.4 - Variation of the solute volume fraction in the isotropic
phase with χ_1, for x = 20, x = 50

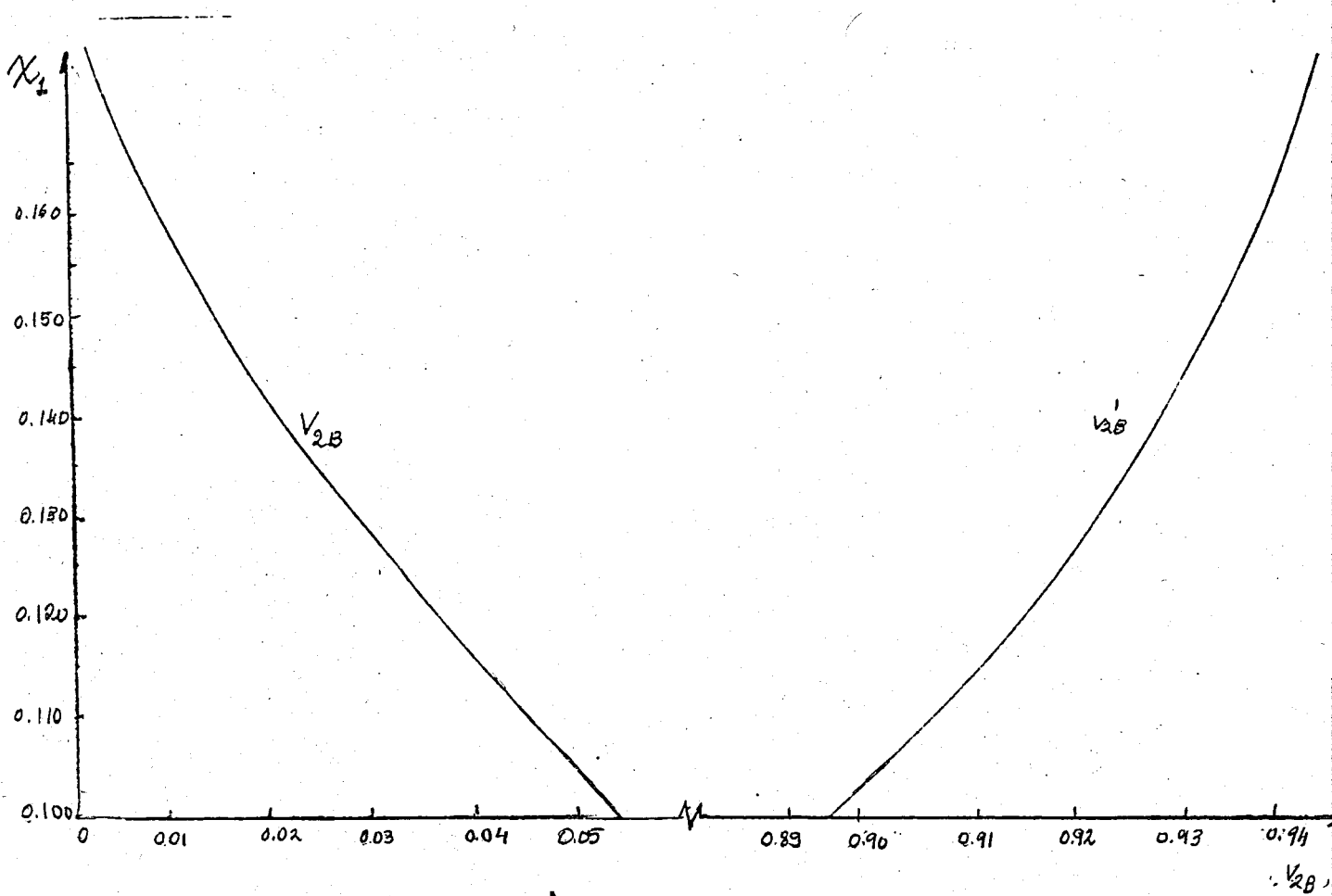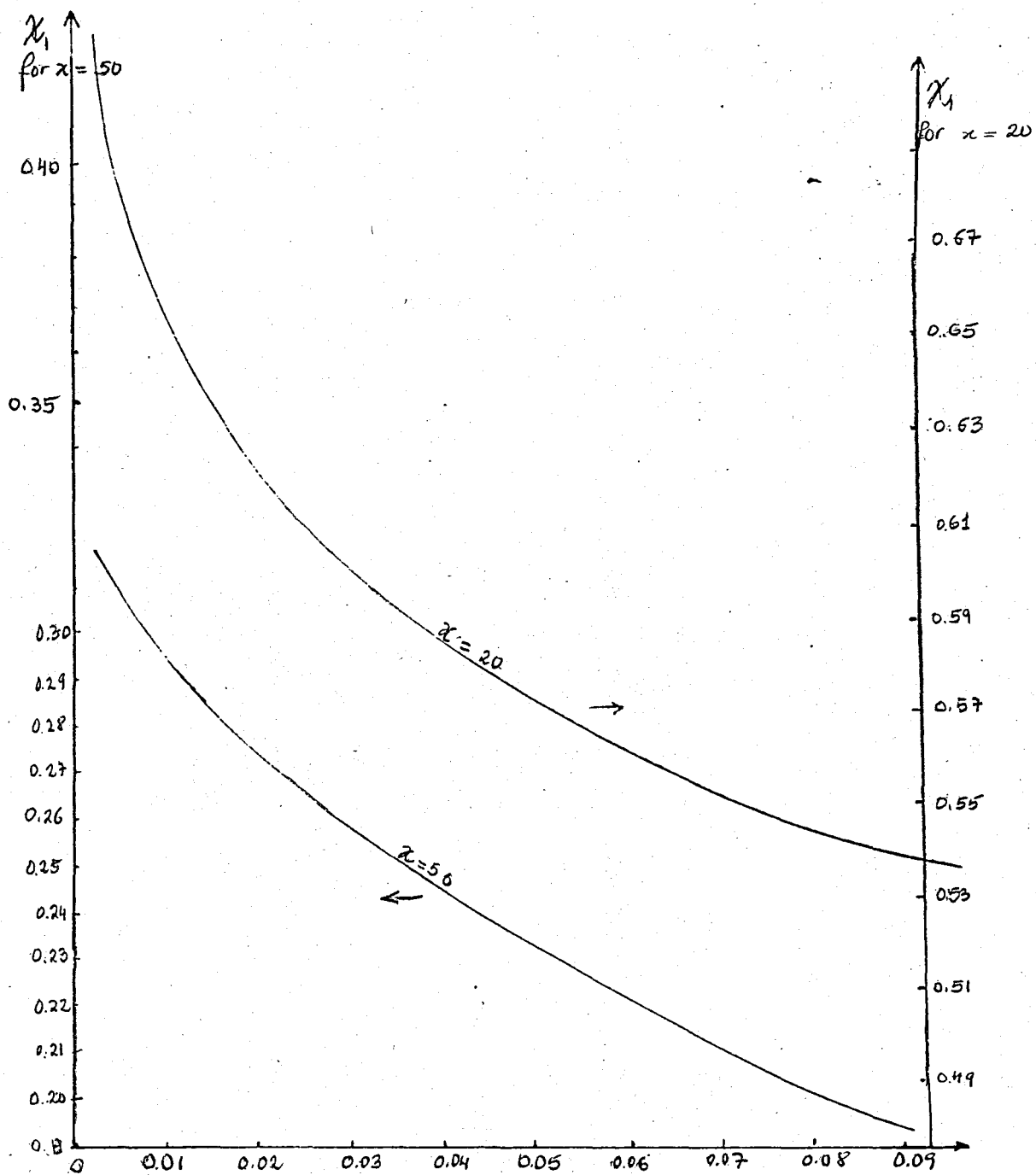As can be seen from the above data the nematic phase is highly concentrated and naturally will exhibit liquid crystalline behaviour.

Now, let us come back to Fig. 4.2. The curves in this figure represent the variation of the macromolecular concentration in the stagnant region (B), with increasing flow rate for a solution with $v_{2A} = 0.01$. These curves may be combined by that of Fig. 4.3 which gives the minimum concentration required for spontaneous appearance of a concentrated nematic phase, for a quiescent solution. By incorporating the data points of Fig. 4.3 within Fig. 4.2, one can separate Fig. 4.2 into two parts, the upper part standing for the two phase equilibrium system and the lower representing points belonging to solely isotropic solution. Hence, dashed line in Fig. 4.2 is obtained directly from Fig. 4.3. From the resulting figures, one can determine the critical values G_c^*, (in the sense that those which give rise to the formation of a nearly crystalline nematic phase in the stationary region) as a function of the solvent-solute interaction parameter X_1, from the intersections of the dashed lines with the constant - X_1 lines. The resulting curve is shown in Fig. 4.5, where G_c^*'s are plotted against the corresponding X_1-parameters.

The next step will be to extend the above theoretical arguments to the case involving rodlike particles of smaller length to width ratio, say $x = 20$ and $x = 50$. Again the solute volume fraction will be $v_{2A} = 0.01$, in the flowing stream. For molecules with $x = 20$, Eq. (3.32) implies that the solution will be totally isotropic for $G^* \leq 2.5 \times 10^{-4}$. We will consider the stress induced diffusion under $G^* = 10^{-4}$, 10^{-5} and 10^{-6} respectively. So the diffusion in this range will be governed by Eq. (4.16), which is applicable to istropic flowing streams only.
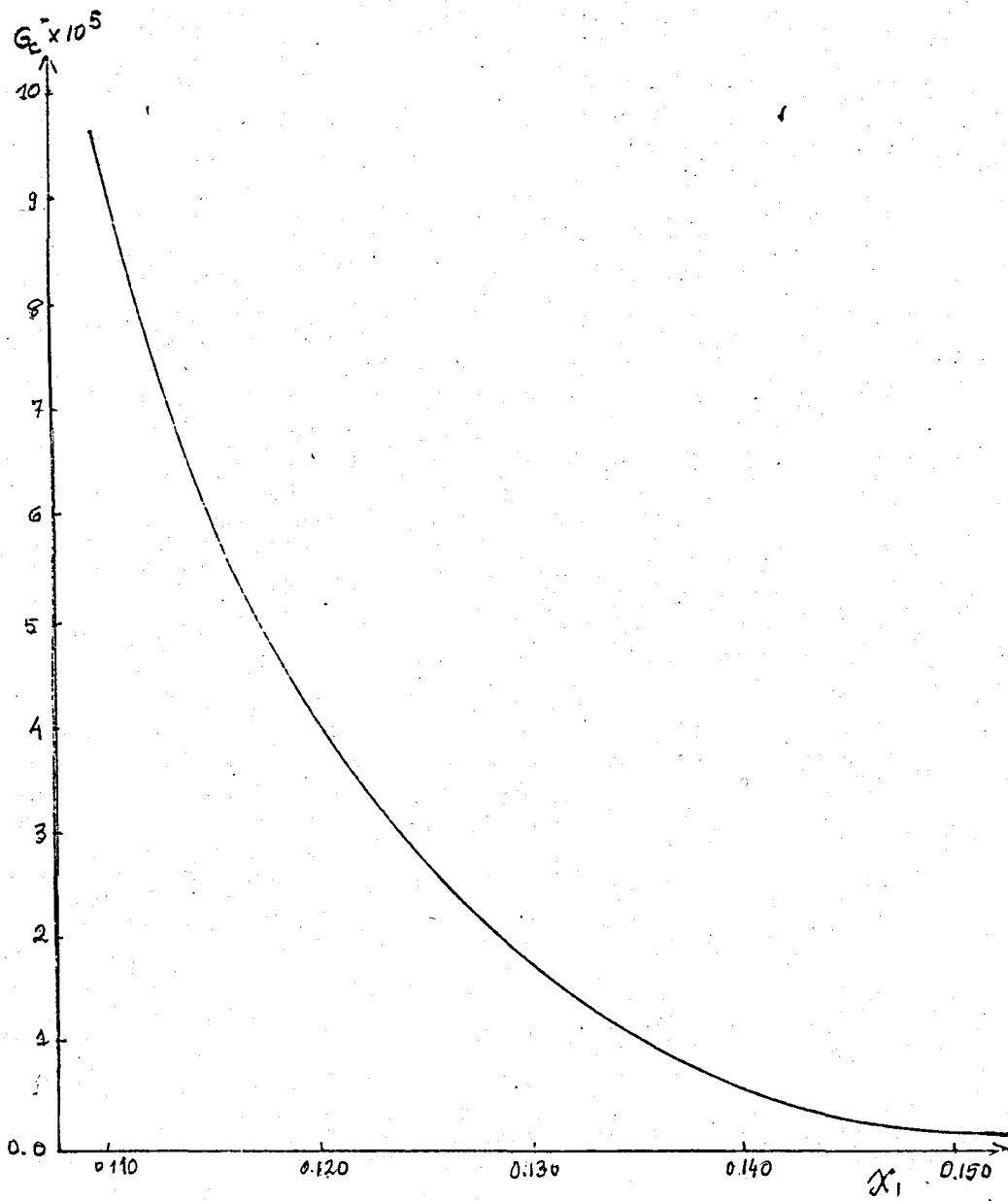
FIGURE 4.5 - G_C^* versus X_1 for x = 100

Again curvers similar to that of x = 100 (See Fig. 4.2) are obtainable; their combination with Fig. 4.4, yields the critical χ_1's that will cause the precipitation of a concentrated nematic phase, for different G values.

Similar calculations were repeated for x = 50. The resulting curves are shown in Fig. 4.6. From these curves, one can verify that, as expected, the contribution of relatively small energy interaction will induce the precipitation of the longest particles under a given flow and gradually as the X-parameter increases, smaller and smaller particles will accumulate. Also, nematic phase formation at stationary regions will be easier in the case of higher flow rate, necessitating the contribution of a relatively small energy interaction parameter compared to lower G^*, especially in the case of longer rods.
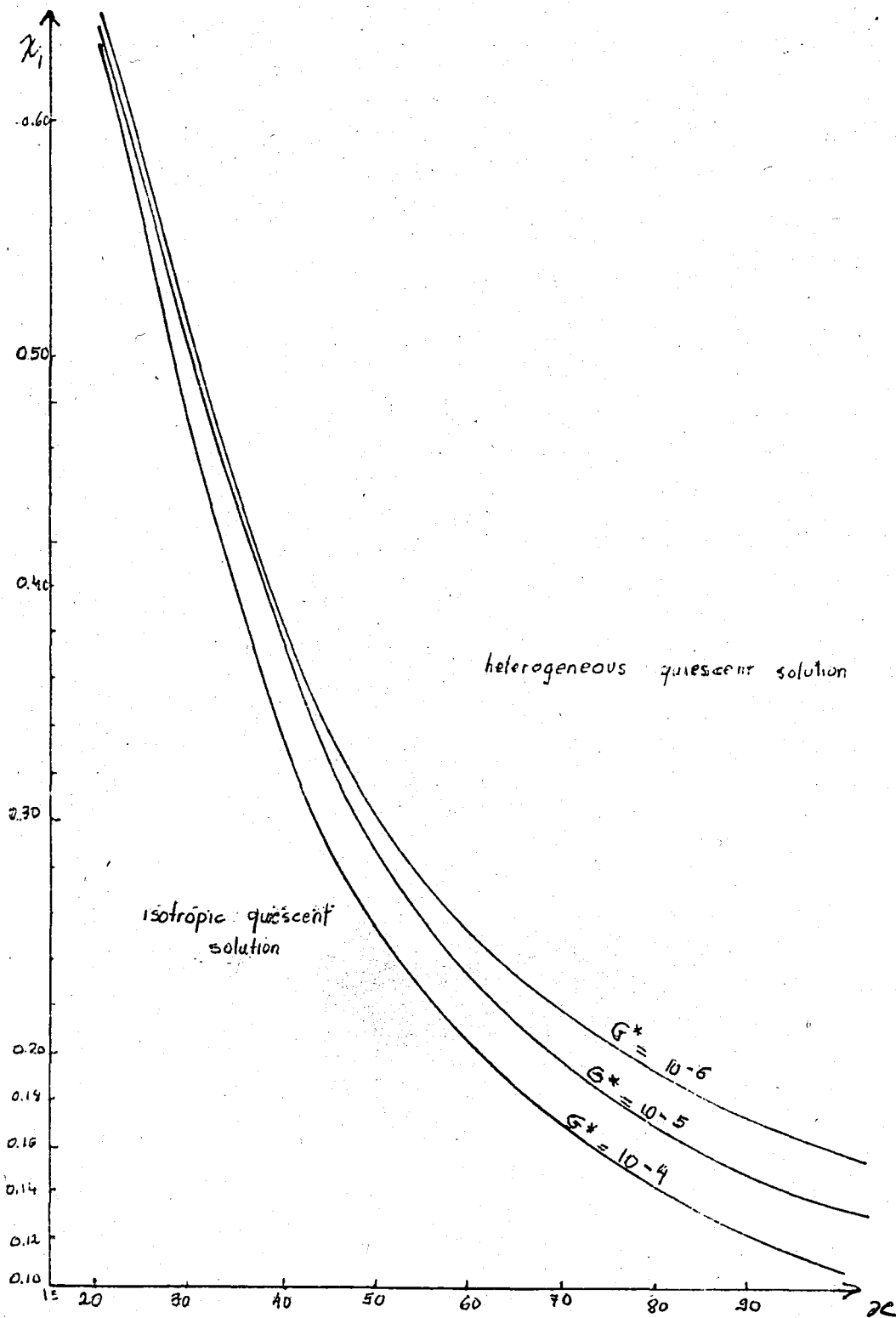
FIGURE 4.6 - Critical X_1's versus axis ratio x, for various $G^{*'}$ s

V. DISCUSSION AND CONCLUSIONS

One purpose of this work was to find an explanation to the aggregation of cholesterol molecules on the inner walls of blood vessels, a phenomenon known as atherosclerosis. Although considerable data on cholesterol metabolism is available, their exact relationship to mechanisms controlling the level of plasma cholesterol or the corresponding rate of deposition are not fully understood. Clinical investigators suggest the need for simpler methods for approaching this problem (Bencze et.al, 1975). In fact, this situation may be explained, to a certain extent on the basis of theoretical arguments presented in the preceeding chapters.

Cholesterol molecules possess rigid rodlike conformation with the exception of a flexible tail that is neglected in the present study. Their volume fraction, together with cholestryl esters and some lipids that forms also liquid crystalline deposits, reaches about 0.01 (Lehninger, 1975). Hence the selection of 0.01 for initial macromolecular concentration in the flowing stream was not arbitrary but followed from the actual concentration of rodlike particles susceptible in giving rise to the formation of a nematic phase along the inner walls of the vessels. On the other hand Poiseuille flow is reasonable for small arteries where relatively high shear rates causes the blood to approach Newtonian rather than Casson behaviour (Lightfoot, 1974). Also near the walls the Poiseuille

flow can be approximated by simple shear flow, so that Eq. (3.19) holds with the dimensionless parameter G^* defined by Eq. (3.30).

Now let us confine our attention to the dimensionless quantity G^* prevailing in blood vessels. The denominator represents the diffusion coefficient of the solute and is in the order of 10^{-7} cm²/sec for all blood lipoproteins (Lehninger, 1975). The segment length of the macromolecule may be taken to be equal to 10 Å. The only remaining unknown, Γ may be calculated from the velocity gradient at the wall. For Poiseuille flow the volume flow rate Q, is given by (Slattery, 1972):

$$Q = -\frac{\pi}{8}\frac{R^4}{\mu}\frac{\partial P}{\partial z} = -\pi\frac{\Delta P}{L}\frac{a^4}{8\mu}$$ (5.1)

where R is the tube radius, μ is the viscosity of the fluid, $\partial P/\partial z$ denotes the pressure drop in the direction of the flow and L is the length of the tube. Also the velocity field is given by

$$v_2 = \frac{\Delta P}{4\mu L}R^2[1 - \frac{r^2}{R^2}]$$ (5.2)

Then $\left.\dfrac{\partial v_z}{\partial r}\right|_{r=R} = -\dfrac{\Delta P R^2}{2\mu L R^2}\left.r\right|_{r=R} = -\dfrac{\Delta P R}{2\mu L}$ (5.3)

Eq. (5.1) yields

$$-\frac{\Delta P}{2\mu L} = \frac{4Q}{\pi R^4}$$ (5.4)

Substituting Eq. (5.4) in Eq. (5.3), we may write

$$\Gamma = \left.\frac{\partial v_2}{\partial r}\right|_{r=R} = \frac{4Q}{\pi R^3}$$ (5.5)

Using $Q = 5.3$ L/min, $R = 0.05$ cm for arterioles (Lightfoot, 1974) we obtain $\Gamma \approx 1000$/sec. Also average capillary radius is in the order of 10^{-4} cm and the corresponding flow velocity is 0.1 cm/sec (Villars, 1974), to obtain again $\Gamma \approx 10^3$/sec. Substituting there data in G^*, we observe that $G^* \approx 10^{-5}$, which is within our domain of calculations.

Calculations carried out in this work indicate that there will be a highly concentrated nematic phase formation in the stagnant parts of a system of rodlike particles subject to homogeneous flow characterized by a G^*, in the order of 10^{-5}, even if the system is very dilute ($v_{2A} = 0.01$), provided that the solvent-solute interaction parameter exceeds a critical value. As stated earlier the migration of macromolecules towards stagnant regions is driven by gradients in entropic potential, i.e. cholesterol molecules have a natural tendency to diffuse to regions of lower stress where the fluid is stagnant due to some possible surface roughness. Recently it has been shown (Huang, 1978) that the growth of atherosclerotic plaques occurs, in fact at certain favored sites and particularly next to surface layers of fibrinogen which causes a surface roughness initiating cholesterol and other lipoproteins accumulation.

Though initially the molecules are randomly distributed in these regions, sufficiently high G^* values, associated with high shear rate may bring the macromolecular concentration in these quiescent locations to attain certain critical levels corresponding to isotropic-nematic equilibrium concentration, with the assistance of a positive solvent-solute interaction. These results are in accordance with Copley's hypothesis (1978) that atherogenesis is strongly influenced by high shear rates at the arterial wall. In fact G^* is factor responsible for the diffusion of macromolecules: the higher the value of G^* (or implicitly Γ), the stronger the diffusion is.

The newly formed anisotropic phase is so concentrated that we may speak of the "precipitation" of a liquid crystalline phase where the building blocks are the cholesterol and its esters. An excessive agglomeration of these molecules may lead to occlusion of blood vessels.

To be more specific, let us consider the case of $G^* = 10^{-5}$, a plausible value for blood flow. Starting with a flowing stream with 1% solute volume fraction, at $\chi_1 = 0.135$, the particles with axis ratio $x = 100$ will be forming a highly concentrated anisotropic phase ($v_{2B}' = 0.9248$) as can be derived from Fig. 4.6. As the χ_1-parameter increases, gradually smaller and smaller particles will precipitate. For example at $\chi_1 = 0.285$, particles with $x = 50$ will undergo phase separation and give rise to an ordered phase with $v_{2B}' = 0.935$.

For shorter rodlike particles ($\sim x < 25$), the variations in the flow rate have a negligible influence on the formation of nematic phase. Here, the appearance of the concentrated ordered phase is brought about by the effect of a sufficiently high interaction energy solely. For example, for rods of $x = 20$ deposition occurs, if χ_1 exceeds ~ 0.63, regardless of the flow rate. Bearing in mind that the precipitating molecules in the blood are relatively short, this property points out the importance of the solute-solvent interaction parameter in nematic phase formation.

The theory presented in this work is applicable to deposits from suspensions or polymer solvent systems in industrial equipment, referred to as the "fouling effect". The tendency of certain fluids to form fouling deposits on heat transfer surfaces is a serious problem in the design of heat-exchange equipment. It is emphasized that some solutes in process streams polymerize and the resulting less soluble material is

deposited on the surface as a film, often of considerable toughness (Bennett, Myers, 1962) this deposit being dependent on both the flow rate and the nature of the fluid, in agreement with the theory presented.

REFERENCES

1.   Bennett, C.O., Myers, J.E., "Momentum, Heat and Mass Transfer",
      Mc Graw-Hill Book Co., Inc., Chem. Eng. Series, 2nd Ed., 1962.

2.   Bencze, W.L., Dempsey, M.E., Eisenberg, S., Frantz, I.D., Hess,R.,
      Kritchevsky, D., Levy, R.I., Miettinen, T.A., Zemplenyi, T.,
      "Hypolipidemic Agents", Editor: D. Kritchevsky, Springer-Verlag,
      Berlin Heidelberg, 1975.

3.   Bird, R.B., Johnson, Jr., M.W., Curtiss, C.F., "Potential Flows
      of Dilute Polymer Solutions by Kramers' Method", Journal of Chem.
      Phys., 51, 7, pp. 3023-3026, 1969.

4.   Bird, R.B., Hassager, O. , Armstrong, R.C. , "Dynamics of Poly-
      meric Liquids", Volume 2, Kinetic Theory, John Wiley and Sons,
      Inc., 1975.

5.   Eringen, C., "Mechanics of Continua", John Wiley and Sons, Inc.,
      1967.

6.   Evans, H.L., "Laminar Boundary Layer Theory", Addison-Wesley
      Publ. Co., 1968.

7.   Flory, P.J., "Principles of Polymer Chemistry", Cornell University
      Press, Ithaca, New York, 1953.

8.   Flory, P.J., "Phase Equilibria in Solution of Rodlike Particles",
      Proceedings of Royal Soc., A, 234, pp. 73-89, 1956.

9.   de Gennes, P.G., "The Physics of Liquid Crystals", Clarendon Press,
      Oxford, 1974.

10.   Gray, G.W., Winsor, P.A., "Liquid Crystals and Solid Crystals",
      Vol. I, John Wiley and Sons, Inc., 1974.

11.   Huang, C.R., Fabisiak, W., "A Rheological Equation Characterizing
      both the Time Dependent and the State Viscosity of Human Blood",
      A.I.ChE Symposium Series, Biorheology, 1979.

12.   Kramers,A.H. , "The Behaviour of Macromolecules in Inhomogeneous
      Flow", Journal of Chem. Phys., 14, 7, 1946.

13.   Lehninger, A.L., "Biochemistry", 2nd Ed., Worth Publications
      Inc., 1975.

14.   Lightfoot, E.N., "Transport Phenomena in Living Systems", John
      Wiley and Sons, 1974.

15. Lipschutz, S., "Theory and Problems of Linear Algebra", Schaum's Outline Series, McGraw-Hill Book Co., Inc., 1968.

16. Marucci, J., Ciferri, A., "Phase Equilibria of Rodlike Molecules in an Extensional Flow Field", Polymer Letters Ed., Journal of Polymer Sciences, 1975.

17. Priestley, E.B., Wojtowicz, P., Sheng, P., "Introduction to Liquid Crystals", Plenum Press, New York - London, 1975.

18. Slattery, J.C., "Momentum, Energy and Mass Transfer in Continua", McGraw-Hill Kogakusha Ltd., 1972.

19. Silebi, C.A., McHugh, A.J., "Effect of Nonhomogeneous Shear Rates on the Flow-Induced Crystallization of Macromolecules", Journal of Polymer Sciences, Pol. Phys. Ed., 17, pp. 1469-1483, 1979.

20. Tirrell, M., Malone, M.F., "Stress-Induced Diffusion of Macro-molecules", Journal of Polymer Science, Polymer Physics Edition, 15, pp. 1569-1583, 1977.

21. Villars, F.M.H., Benedek, G.B., "Physics with Illustrative Examples from Medicine and Biology", Vol. 2, Statistical Physics, Addison-Wesley Co., 1974.

22. Warner, M., Flory, P.J., "The Phase Equilibria in Thermotropic Liquid Crystalline Systems", Journal of Chem. Phys., 73, 12, pp. 6327-6332, 1980.

APPENDICES

A.I. DERIVATION OF ΔG_m FOR SOLUTIONS OF RODLIKE PARTICLES

Let j solute molecules be assigned locations in the volume to be occupied by the solution. The specified distribution of their orientations will be assumed to be symmetrical about an axis. We shall estimate the number ν_{j+1} of situations available to an additional molecule, $j+1$, oriented at an angle ψ_{j+1} to this axis. Each molecule will be replaced by submolecules such that a molecule i inclined at an angle ψ_i to the orientation axis, will be divided into y_i submolecules. The width of a submolecule is chosen to be equal to ℓ/x where ℓ is the total length of the molecule and x is the total number of segments in the molecule.

As can be seen from the Fig. A.1 {the number of submolecules y_i per molecule i} = $(\ell \sin \psi_i)/(\ell/x) = y_i$ or $y_i/x_i = \sin \psi_i$. Obviously, each submolecule contains x/y_i segments and requires therefore, x/y_i vacant lattice sites.

The number of sites available to the first segment of the first submolecule of $(j+1)$'th molecule = $(n_0 - xj)$ where n_0 is the total number of lattice sites.

Considering the vacancies and the submolecules as two sets arranged in random linear sequence, the probability that the subsequent segment of the first submolecule is given by:
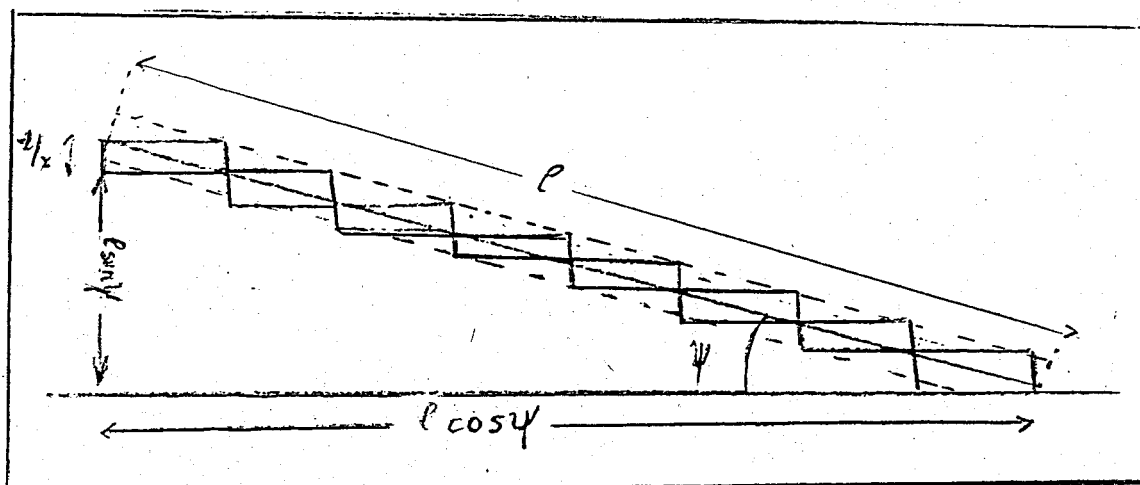
FIGURE A.1 - Schematic representation of a rodlike
macromolecule

$$\frac{\text{number of vacant sites}}{\text{number of vacant sites} + \text{number of submolecules}} = \{\frac{n_0 - xj}{n_0 - xj + \sum\limits_{i=1}^{j} y_i}\} \quad (A.1)$$

For all the segments of the first submolecule, this probability becomes

$$\{\frac{n_0 - xj}{n_0 - xj + \sum\limits_{i=1}^{j} y_i}\}^{((x/y) - 1)} \quad (A.2)$$

since there are $((x/y_{j+1}) - 1)$ remaining segments in the first submolecule.
Now, let's consider the second submolecule; the probability of vacancy of
lattice site for the first segment, equals

$$\left(\frac{n_0 - xj}{n_0}\right) \qquad (A.3)$$

and that for all its remaining segments is given by the same expression as in (A.2). Since there are $y_{j+1} - 1$ submolecules, the product of (A.2) and (A.3) should be raised to the power $(y_{j+1} - 1)$, so that the final expression will be:

$$\nu_{j+1} = (n_0 - xj) \frac{n_0 - xj}{(n_0 - xj)\sum\limits_{i=1}^{j} y_i} (x-y_{j+1})$$

$$\left(\frac{n_0 - xj}{n_0}\right)^{y_{j+1} - 1} \qquad (A.4)$$

Upon rearrangement and using $y = \sum\limits_{i=1}^{j} y_i / j$, we obtain,

$$\nu_{j+1} = \frac{(n_0 - xj)^x}{(n_0 - xj + yj)^{x-y_{j+1}} \, n_0^{(y_{j+1}-1)}} \qquad (A.5)$$

The expression for the partition function of an isotropic solution consisting of n_1 solvent molecules and n_2 solute molecules is given by

$$Q_m = q_1^{n_1} q_2^{n_2} \prod_{j=1}^{n_2} \nu_j / \prod_k n_k = q_1^{n_1} q_2^{n_2} \Omega \qquad (A.6)$$

where q_1, q_2 are the internal partition functions for molecules 1 and 2, and n_k whose directions occur within the solid angle $\delta\omega_k$. Hence we will insert the expression (5) into the Eq. (6). To get a more concise expression we use the approximation:

$$(n_0 - xi)^x = \frac{(n_0 - xi)!}{[n_0 - x(i + 1)]}$$

$$\Rightarrow \prod_{j=1}^{n_2} (n_0 - xj)^x = \frac{(n_0)!}{(n_0 - n_2 x)!}$$

to obtain finally,

$$Q_m = q_1^{n_1} \; q_2^{n_2} [\frac{(n_1 + yn_2)!}{n_1! n_2! (n_1 + xn_2)^{(y-1)n_2}}] \; \frac{n_2!}{\prod_k n_k!} \tag{A.7}$$

In the above expression $n_2!/\prod_k n_k!$ corresponds to the number of orientations each solute may choose, and is equal to y^{2n_2} (Flory, 1956) so that Ω = probability or number of ways of arrangements of solute molecules within the mixture is found to be:

$$\Omega = \frac{(n_1 + yn_2)!}{n_1! n_2! (n_1 + xn_2)^{(y-1)n_2}} \; y^{2n_2} \tag{A.8}$$

Using Stirling approximation ($\ln n! = n \ln n - n$), we get, after some algebraic manipulations:

$$\ln \Omega = n_1 \ln v_1 + n_2 \ln v_2 - (n_1 + yn_2) \ln[1 - v_2(1 - y/x)]$$

$$- n_2 [\ln(xy^2) - y + 1] \tag{A.9}$$

where
$$v_2 = \frac{xn_2}{n_1 + xn_2}$$

$$v_1 = \frac{n_1}{n_1 + xn_2}$$

are the respective volume fractions.

Inserting the expression (A.9) into the Boltzmann Equation

$$\Delta S_m = k \ln \Omega \qquad (A.10)$$

we obtain the change in entropy upon mixing. This term includes only configurational entropy change, the one associated with the entropy change due to interaction between unlike pairs being implicitly contained in the Van Laar expression for ΔH_m: consider the change in energy associated with breaking 1/2 pairs of solvent and polymer bonds, each, and joining one [1,2] bond. This may be formulated as:

$$\Delta\omega_{12} = \omega_{12} - \frac{1}{2}\omega_{11} - \frac{1}{2}\omega_{22}$$

where ω's refer to the energies associated with these respective bonds. This energy includes the heat of mixing and, if there is, the energy related with interactional entropy change, i.e. $\Delta\omega_{12} = \Delta\omega_h - T\Delta\omega_s$. The average value of the number of [1,2] contacts in a solution containing n_2 polymer molecules, with x segments each and z coordination number, is

$$\{n_2[(z-2)x+2]\}[v_1] \qquad (A.11)$$

where $(z-2)x+2$ = number of neighboring sites/molecule

v_1 = mole fraction of solvent = probability that this

neighboring site will be a molecule of a solvent.

The quantity labelled (11) is approximately equal to

$$\{n_2 z x v_1\} \quad \text{or} \quad \{n_1 z v_2\}$$

so that ΔH_m = {total number of [1,2] contacts}{energy associated with each contact}

$$= n_2 z x v_1)(\Delta\omega_{12}) \qquad (A.12)$$

If we define $X_1 = z\Delta\omega_{12}/kT$, $\qquad (A.13)$

substituting Eq. (A.13) in Eq. (A.12) yields the well-known Van Laar expression:

$$\Delta H_m = kTX_1 n_1 v_2 = kTX_1 xn_2 v_1 \tag{A.14}$$

By definition, $\Delta G_m = \Delta H_m - T\Delta S_m$ \hfill (A.15)

Combining Eqs. (A.9), (A.10), (A.14) and (A.15), we get the final expression for the Gibbs free energy of mixing:

$$\frac{\Delta G_m}{kT} = n_1 \ln v_1 + n_2 \ln v_2 - (n_1 + yn_2)\ln[1 - yv_2(1 - y/x)]$$
$$- n_2[\ln(xy^2) - y + 1] + X_1 xn_2 v_1 \tag{A.16}$$

A.2. CALCULATION OF $<\sin \psi>$ AND $<\sin^2 \psi>$

$$\frac{y}{x} = <\sin\psi> \equiv \frac{\int_0^{2\pi} \int_0^{\psi} \sin^2\psi \, d\psi \, d\theta}{\int_0^{2\pi} \int_0^{\psi} \sin\psi \, d\psi \, d\theta} = \frac{\psi/2 - (1/2)\sin\psi \cos\psi}{1 - \cos\psi} \quad (A.17)$$

$$<\sin^2\psi> = \frac{\int_0^{\psi} \sin^3\psi \, d\psi}{\int_0^{\psi} \sin\psi \, d\psi}$$

$$= \frac{[-(\cos\psi \sin^2\psi)/3 + (2/3)[-\cos\psi]] \Big|_0^{\psi}}{1 - \cos\psi}$$

$$= \frac{(1/3)[-\cos\psi][\sin^2\psi + 2] + (2/3)}{1 - \cos\psi} \quad (A.18)$$

By making use of Eq. (A.17) and (A.18), the following table may be calculated:

$\psi(o)$	$<\sin \psi>$ or y/x	$(<\sin\psi>)^2$ or $(y/x)^2$	$<\sin^2\psi>$
0	0	0	0
15	0.173	0.030	0.034
30	0.338	0.114	0.128
45	0.487	0.237	0.264
60	0.614	0.373	0.417
75	0.712	0.507	0.558
90(random)	0.7854	0.616	0.667

For random distribution, $<\sin\psi> = <\sin \pi/2>$ or $y/x = \pi/4 = 0.7854$. But Flory took $y/x \simeq 1$, for convenience.

Also as can be seen from the above table, taking $<\sin^2\psi> \simeq (y/x)^2$ is an acceptable approximation.

A.3. DERIVATION OF THE DIRECTION OF
THE NEMATIC AXIS

Let's consider $\underset{\approx}{k}$, the velocity gradient tensor

$$\underset{\approx}{k} = \begin{vmatrix} k_{11} & k_{12} & k_{13} \\ k_{21} & k_{22} & k_{23} \\ k_{31} & k_{32} & k_{33} \end{vmatrix}$$

for irrotational flow we must have $\underset{\approx}{k}$ symmetrical or it must be diagonal matrice.

To diagonalize $\underset{\approx}{k}$, an orthogonal transformation matrix P such that $\underset{\approx}{P}^T \underset{\approx}{k} \underset{\approx}{P}$ is diagonal, has to be found. The procedure is as follows:

1) Find the characteristic polynomial $\Delta(t)$ of $\underset{\approx}{k}$

2) Find the eigenvalues of $\underset{\approx}{k}$ (that satisfy the characteristic equation)

3) Find the eigenvectors, substituting the eigenvalues in the matrix $t\underset{\approx}{I} - \underset{\approx}{k}$, where t_i's are the eigenvalues

4) Normalize the eigenvectors

5) $\underset{\approx}{P}$ is the matrix whose columns are the eigenvectors.

The above procedure is illustrated by the example of simple shear flow:

$$\underset{\approx}{k} = \begin{pmatrix} 0 & \Gamma/2 & 0 \\ \Gamma/2 & 0 & 0 \\ 0 & 0 & 0 \end{pmatrix}$$

(1) $\quad \Delta(t) = \left| t\underset{\approx}{I} - \underset{\approx}{k} \right| = \begin{vmatrix} t & \Gamma/2 & 0 \\ \Gamma/2 & t & 0 \\ 0 & 0 & t \end{vmatrix} = t(t^2 - (1/4)\Gamma^2) = 0$

(2) $\quad t_1 = -(1/2)\Gamma$

$\quad\quad t_2 = +(1/2)\Gamma$

$\quad\quad t_3 = 0$

(3) $\quad t_1 = -1/2\Gamma \quad \begin{vmatrix} -1/2\Gamma & 1/2\Gamma & 0 \\ 1/2\Gamma & -1/2\Gamma & 0 \\ 0 & 0 & -1/2\Gamma \end{vmatrix} \begin{vmatrix} x \\ y \\ z \end{vmatrix}_1 = \begin{vmatrix} 0 \\ 0 \\ 0 \end{vmatrix}$

$-1/2\Gamma\, x + 1/2\, \Gamma y = 0$

$\quad\quad\quad - 1/2\, \Gamma z = 0 \quad\quad (x,y,z)_1 = (1 , 1 , 0)$

$t_2 = +1/2\Gamma \quad \begin{vmatrix} 1/2\Gamma & 1/2\Gamma & 0 \\ 1/2\Gamma & 1/2\Gamma & 0 \\ 0 & 0 & 1/2\Gamma \end{vmatrix} \begin{vmatrix} x \\ y \\ z \end{vmatrix}_2 = \begin{vmatrix} 0 \\ 0 \\ 0 \end{vmatrix}$

$1/2(\Gamma x + \Gamma y) = 0$

$\quad\quad\quad \Gamma z = 0 \quad\quad (x,y,z)_2 = (1 , -1 , 0)$

$$t_3 = 0 \qquad 1/2\ \Gamma y = 0$$

$$1/2\ \Gamma x = 0 \qquad (x,y,z)_3 = (0,0,\text{constant})$$

$$0 = 0$$

4) $\qquad (x,y,z)_1 = \underset{\sim}{u}_1 = (1/\sqrt{2}\ ,\quad 1/\sqrt{2},\quad 0)$

$\qquad (x,y,z)_2 = \underset{\sim}{u}_2 = (-1/\sqrt{2},\quad 1/\sqrt{2},\quad 0)$

$\qquad (x,y,z)_3 = \underset{\sim}{u}_3 = (0\quad,\quad\quad 0\ ,\quad 1)$

5) $\qquad \underset{\approx}{P} = \begin{vmatrix} 1/\sqrt{2} & -1/\sqrt{2} & 0 \\ 1/\sqrt{2} & +1/\sqrt{2} & 0 \\ 0 & 0 & 1 \end{vmatrix}$

But $\qquad \underset{\approx}{P} = \begin{vmatrix} \cos\psi & -\sin\psi & 0 \\ \sin\psi & \cos\psi & 0 \\ 0 & 0 & 1 \end{vmatrix}$ $\qquad$ (general form for every orthogonal matrix $\underset{\approx}{P}$ for which det $(\underset{\approx}{P}) = 1$)

Comparison of the last two equalities yields $\psi = \pi/4\ (=45^\circ)$.

A.4. SAMPLE CALCULATION FOR FIGURE 4.2

Figure 4.2 was drawn by simultaneous solution of Eq. (3.31) and Eq. (4.17), by making use of a programmable calculator.

The program includes the following steps.

1) Give x, x_1, v_{2B}, G

2) Assume y

3) Substitute y in Eq. (3.33). Evaluate the righthandside (RHS) of the equation and compare with the lefthandside (LHS) (v_{2A})

4) If %error $(\delta(y))$ is high go to (2). If $\delta(y) < 10^{-4}$ continue.

5) Calculate LHS of Eq. (4.17).

6) Assume v_{2B}

7) Substitute RHS of Eq. (4.17)   If $((RHS - LHS)/RHS) \times 100$ ($\simeq \%\delta(v_{2B})$), exceeds 0.01, go to (6)

8) Stop.

With the above sequence one can easily compute, v_{2B}, corresponding to any x, x_1, v_{2A}, G,

An example is shown below:

⟵ Selected data points ⟶				Assumption			Assumption		
G	x	X_1	v_{2A}	y	$\varepsilon(y)$	LHS (4.17)	v_{2B}	RHS (4.17)	% error
10^-	100	0	0.01	14	-6.68×10^{-3}				
				13.8	-1.99×10^{-3}				
				13.7	3.65×10^{-4}				
				13.74	-5.7×10^{-4}				
				13.71	1.29×10^{-4}				
				13.72	-1.06×10^{-4}				
				13.715	1.00×10^{-5}				
						-18.98	0.04	-19.22	1.27
							0.045	-18.73	-1.32
							0.0422	-18.88	0.1
							0.0423	-18.99	0.05
							0.0424	-18.98	0.00

Hence for $G = 10^{-4}$

$\left. \begin{array}{l} x = 100 \\ X_1 = 0 \\ v_{2A} = 0.01 \end{array} \right\} \longrightarrow v_{2B} = 0.0424$

(with $y = 13.715$ in the A region)